Characterization of Triacylglyceride Lipase and Mono- and Diacylglycerol Acyltransferases in *Manduca sexta*

By

ZENGYING WU

Bachelor of Medicine in Medicine
Nankai University
Tianjin, China
2009

Master of Medicine in Medicine
Nankai University
Tianjin, China
2009

Submitted to the Faculty of the
Graduate College of the
Oklahoma State University
in partial fulfillment of
the requirements for
the Degree of
DOCTOR OF PHILOSOPHY
July, 2014

Characterization of Triacylglyceride Lipase and Mono- and Diacylglycerol Acyltransferases in *Manduca sexta*

Dissertation Approved:

Jose Soulages

Dissertation Adviser

Estela Arrese

Robert Matts

Haobo Jiang

ACKNOWLEDGEMENTS

My deepest gratitude goes first and foremost to my advisors Drs. Jose L. Soulages and Estela Arrese, for their constant support and guidance. Without that, the research work could not be completed successfully and this thesis could not have reached its present form.

Secondly, I should give my hearty thanks to my committee members: Dr. Matts and Dr. Jiang for their sound advice and helpful discussions.

I also owe my sincere gratitude to the lab members - Dr. Alisha Smith, Dr. Soreiyu Umezu, Xiao Chen, Sarah Firdaus and Fredy Saudale who gave me their patience and help to my experiments.

I also want to thank the office and core facility staff of BMB department for their support in my research work.

Lastly, my thanks would go to my beloved family for their loving considerations and great confidence in me all through these years.

Name: ZENGYING WU

Date of Degree: JULY, 2014

Title of Study: CHARACTERIZATION OF TRIACYLGLYCERIDE LIPASE AND MONO- AND DIACYLGLYCEROL ACYLTRANSFERASE IN *MANDUCA SEXTA*

Major Field: Biochemistry and Molecular Biology

Abstract:
Triglyceride (TG) is the main form of lipid storage in the cell. The processes of hydrolysis and synthesis of TG play critical roles the lipid metabolism. Triglyceride-lipase(TGL) is a major fat body lipase hydrolyzing TG in *Manduca sexta*. A WWE domain, presumably involved in protein-protein interactions, has been previously identified in the N-terminal region of TGL. So we searched for proteins partners that interact with the N-terminal region of TGL. Thirteen proteins were identified by mass spectrometry. The oxidoreductase lipoamide-dehydrogenase (LipDH) and the apolipoprotein components of the lipid transporter, HDLp, were among these proteins. LipDH is the common component of the mitochondrial α-keto acid dehydrogenase complexes whereas HDLp occurs in the hemolymph. However, subcellular fractionation demonstrated these two proteins are relatively abundant in the soluble fraction of fat body adipocytes. TGL has critical thiol groups and studies with inhibitors suggested that LipDH, acting as a diaphorase could preserve the activity of TGL by controlling the redox state of thiol groups. The HDLp-TGL interaction affected the catalytic properties of TGL leading to a lower rate of hydrolysis of diacylglycerol (DG).
Monoacylglycerol acyltransferase (MGAT) and diacylglycerol acyltransferase (DGAT) are key enzymes of the synthesis of neutral glycerides. Very little is known about these acyltransferases in insects. We have cloned two predicted MGATs and a DGAT from M. sexta and compared their sequences with predicted MGAT and DGAT homologues from a number of insect species. The comparison suggested that insects may only have a single DGAT gene, DGAT1 and insects seem to have a single MGAT gene which is similar to the MGAT2 of vertebrates. Furthermore, the expression patterns of the acyltransferases suggest a significant role of the monoacylglycerol pathway in the production and mobilization of DG in M. sexta fat body.

TABLE OF CONTENTS

Chapter Page

I. INTRODUCTION 1

II. TGL-mediated lipolysis in *Manduca sexta* fat body: Possible roles for lipoamide-dehydrogenase (LipDH) and high-density lipophorin (HDLp) 8

Introduction.....8
Experiment Procedures 10
Results and Discussion 18

III. Study of Mono- and Diacylglycerol Acyltransferases in *Manduca sexta* 39

Introduction.....39
Experiment Procedures 41
Results and Discussion 42

LIST OF TABLES

Table Page

Table 1 WWE interacting proteins identified by MS/MS 22

Table 2 Identity Matrix, Masses and Isoelectric points of DGAT1 46.....44

Table 3 Identity matrix of insect, human and mouse proteins from the DGAT2 family58

LIST OF FIGURES

Figure Page

Figure 1 *Manduca sexta* life cycle 3

Figure 2 Sketch of TGL structure showing key conserved residues and structural regions 4

Figure 3 Schematic overview of lipid mobilization and transport in M. sexta during flight activity.....5

Figure 4 Triacylglycerol synthesis and acyl-CoA:diacylglycerol acyltransferase (DGAT) enzymes.....7

Figure 5 Sequence, Expression and Circular Dichroism of N-terminal region of TGL20

Figure 6 WWE Interacting Proteins Assay 22

Figure 7 Co-immunoprecipitation of TGL with anti-HDLp antibodies 24

Figure 8 Subcellular Localization of LipDH in M. sexta Fat Body.....27

Figure 9 Effect of DTT, GSH, GSSG and NEM on TGL Activity 29

Figure 10 Effect of Carmustine (A) and Auranofin (B) on lipase activity 31

Figure 11 Effect of AKH on lipase activity in the presence and absence of reducing agents 33

Figure 12 Subcellular distribution of lipophorin, DG and TG.....35

Figure 13 Effect of lipophorin on the lipase activity of TGL 38

Figure 14 DNA and protein sequence of MsexDGAT1 45

Figure 15 Sequence alignment of Human DGAT1 (NP_036211.2) and MsexDGAT1 (KF800701).....46

Figure 16 Multiple sequence alignment of insect proteins similar to Manduca DGAT1 50

Figure 17 Multiple sequence alignment DGAT1 from Lepidoptera 51

Figure 18 Conserved Phosphorylation Sites Among DGAT1 52

Figure 19 Structure of DGAT1 genes.....54

Figure 20 Features of MsexMGAT gene and protein structure.....62

Figure 21 Structure of MGAT genes 64

Figure 22 Protein sequence alignment of Human and mouse MGAT2 and MsexMGATs 66

CHAPTER I

Introduction

Insects provide a wide range of benefits to humanity. Most of our crops are dependent on pollination by insects, and the production of meat and milk depend on pollinated plants that are eaten by domestic animals[1]. In many parts of the world, people utilize insects as a source of food with significant amount of protein. Insects were among the earliest animals that appeared on earth, and many of the insects we know today are descended from ancestors that came into being even before the Mesozoic era, which can be seen in the one of the oldest fossils[2]. The metabolic rate of some insects, especially flying insects is among the highest known in nature[3]. Such a high metabolic rate and the considerable short life span make insects great models for the study of metabolic pathways that are often highly conserved throughout the animal kingdom.

Lipolysis is the process of hydrolysis of triacylglyceride into glycerol and free fatty acids. Lipolysis is a central metabolic process. In insects lipolysis provides energy for flight. To Manduca sexta and most of the long-distance flying insects, direct utilization of fat reserves in fat body has been shown to be the main source of energy.[4] Neutral lipids in the form of triglycerides [5] are the predominant form of storage of fatty acids and comprise the main energy reserve in insects and all other animals. Insects accumulate TG as lipid droplets within the cytoplasm of fat body cells during feeding periods.

The fat body is the adipose tissue where majority of lipid is stored.[6]. The insects rely on the reserves in fat body to support the energy requirements associated to non-feeding periods, sustained flight and embryo development. Storage of fatty acids is essential in insects for other functions as well. Fatty acids serve as precursors in the synthesis of waxes and pheromones, and as components of cuticular lipids in addition to participate in phospholipid synthesis for membrane biogenesis and synthesis of eicosanoids. Insects contain a lot of fat bodies. These fat bodies are not just the storage sites of lipids, but in fact also centers of growth, development, metamorphosis and reproductive activity. Due to the function of nutrition storage, detoxification and insect life cycle activities metabolite biosynthesis, the fat body of the insect is actually a combination of adipose tissue and vertebrate liver: the center of lipid metabolism.

Our lab uses *Manduca sexta* as an insect model to study lipid metabolism. M .sexta, the tobacco hornworm, , is a moth with three different life stages: the larva, pupa, and adult (Figure 1).In the larval stage, the content of TG in the fat body increases from a few mg to ~80 mg [6]. While during subsequent development, the lipid reserves are used to sustain the life of the adult insect, which feeds occasionally [7]. M. sexta represents an excellent model for studying the basic mechanisms involved in the mobilization of TG in insects.

Figure 1. ***Manduca sexta*** **life cycle**

(Source: http://insected.arizona.edu/manduca/Mand_cycle.html)

TG is stored in fat body adipocytes as cytosolic lipid droplets. TG hydrolysis (lipolysis) is mediated by a TG-lipase The TG-lipase has been purified from the cytosol[8], and it is the only lipase purified and characterized in insect so far. TGL is a polypeptide with a relative mass of 74-76kDa that has been identified as the homolog of D. melanogaster CG8552 The end-product of insect lipolysis is sn-1,2-diacylglycerol (DG) that is released into the hemolymph [10, 11]

The main triglyceride lipase found in the fat body of insects was cloned, sequenced, and expressed in our lab. TGL cDNA from M. sexta was cloned using RT-PCR methods and cDNA synthesized from fat body mRNA. MsTGL cDNA is 2246bp long and contains an open reading frame (ORF) of 1950 bp that encodes a 649 amino acid protein with a theoretical molecular weight of 73.8 kDa and an isoelectric point of 5.5. The ORF ends at position 2044 and is

followed by a 202 -nucleotide 3'-untranslated region including a poly(A) tail of 21 residues. Two copies of the potential polyadenylation signal are found at positions 2200 and 2238, respectively.

A comparison of the deduced MsTGL protein sequence with the sequences of other putative insect TGLs (CG8552-like) shows significant conservation (~ 53% amino acid identity). The conservation is particularly high in three regions where potential functional domains are found: the N-terminal region that contains a WWE domain (amino acids 46 to 128), the central region in which the lipase consensus sequence (GHSLG) containing the active site serine (Ser 367) is located, and the C-terminal region that contains the DDHD domain (amino acids 411 to 609).

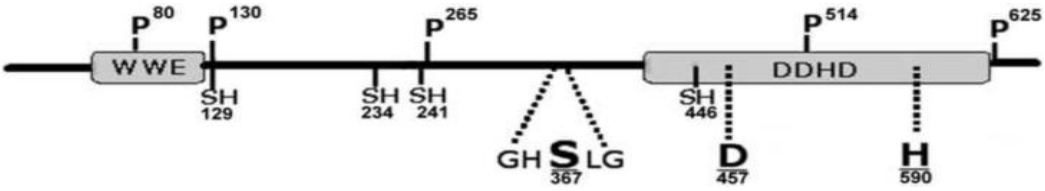

Figure 2 Sketch of TGL structure showing key conserved residues and structural regions. The figure shows the locations of conserved Cys residues and phosphorylation sites present in insect TGLs. It also shows the predicted catalytic triad comprising the serine residue within the GHSLG sequence (366S) and the conserved aspartic (457D) and histidine (590H) located in the DDHD domain.

TGL shares significant sequence similarity with vertebrate phospholipases from the phosphatidic acid phospholipase A1 (PAPLA1) family [9]. TGL is well conserved among insects [9]. The enzyme can catalyze the hydrolysis of tri-, di-, and mono-acylglycerols, but shows highest affinity for tri- or di- acylglycerol. The fat body lipase exhibits a preference for hydrolyzing the primary ester bonds of acylglycerols, and does not show stereoselectivity toward either the sn-1 or sn-3 position of trioleoylglycerol. Its activity has an optimum pH (7.9) and can be inhibited by diisopropylfluorophosphate, ATP, ADP, Mg2+, and NaF [8]. In addition to its

main triglyceride and diglyceride hydrolase activities, TGL has a significant phospholipase A1 activity [9] with the ability to hydrolyze the phospholipids of the outer layer of the LDs. This activity is expected to facilitate the access of TGL to the core of the LDs where TG molecules localize. TG hydrolysis necessarily involves the interaction of the lipase with the lipid droplet. However, TGL does not achieve a tight association with the LDs and experimentally is only found in the cytosol regardless of the lipolytic conditions [12]. TGL is constitutively phosphorylated in vivo, and its phosphorylation level is unchanged by AKH, the main lipolytic hormone of insects [13].

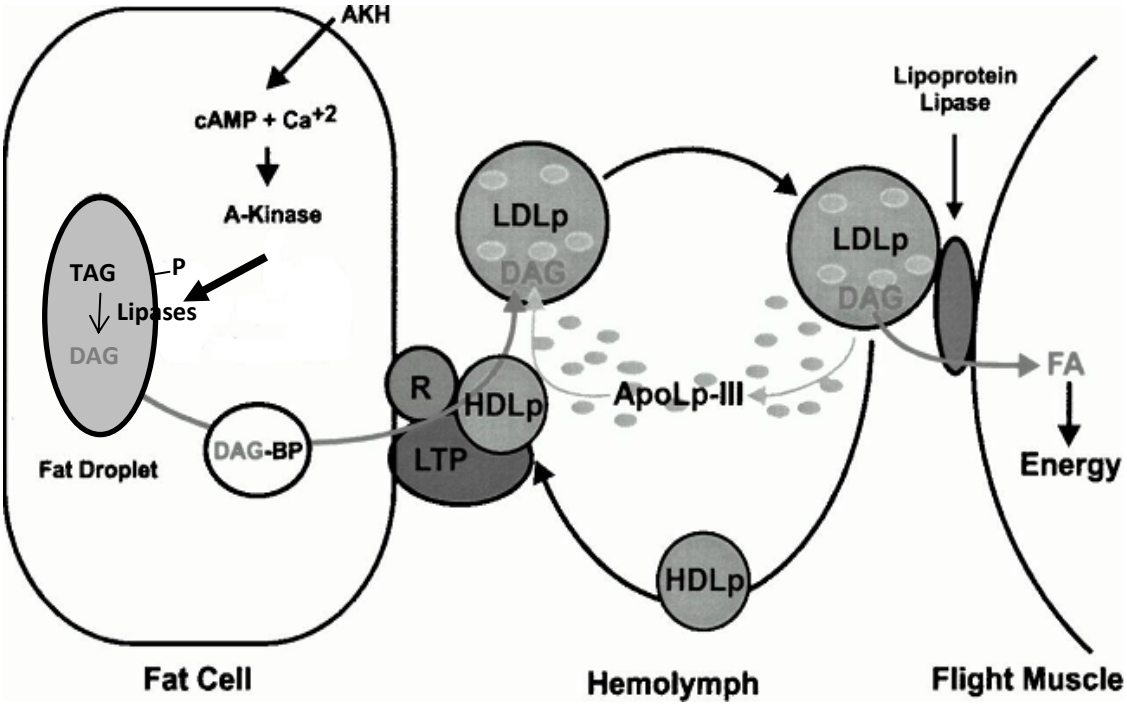

Figure 3. Schematic overview of lipid mobilization and transport in M. sexta during flight activity (Source: Canavosa et al., 2001)

TG synthesis is as significant as lipolysis in the metabolism of TG. In addition to energy storage, TG synthesis in cells may protect them from the potentially toxic effects of excess FA. There are

two known major pathways for TG biosynthesis: the glycerol phosphate or Kennedy pathway[29] and the monoacylglycerol (MG) pathway[30, 31]. In these two pathways fatty acyl-CoAs are utilized by intracellular acyl-CoA synthases[32]. The Kennedy pathway is present in most cells, whereas, the MG pathway exists in specific cell types, such as enterocytes, hepatocytes, and adipocytes, where it may participate in the reesterification of hydrolyzed TG[33]. In the final reaction of both pathways, a fatty acyl-CoA and diacylglycerol (DG) molecule are covalently joined to form TG. Such reaction is catalyzed by acyl-CoA:diacylglycerol acyltransferase (DGAT) enzymes. The newly synthesized TGs are believed to be released into the associated lipid bilayer, from where they are transported into cytosolic lipid droplets[34]. DGAT is found to be bound to the ER membrane[35]. Diacylglycerol lies at the branch point between phospholipid and storage-lipid synthesis and DGAT catalyses the final acylation of the Kennedy pathway and is the only step in the pathway unique to TAG synthesis[36].

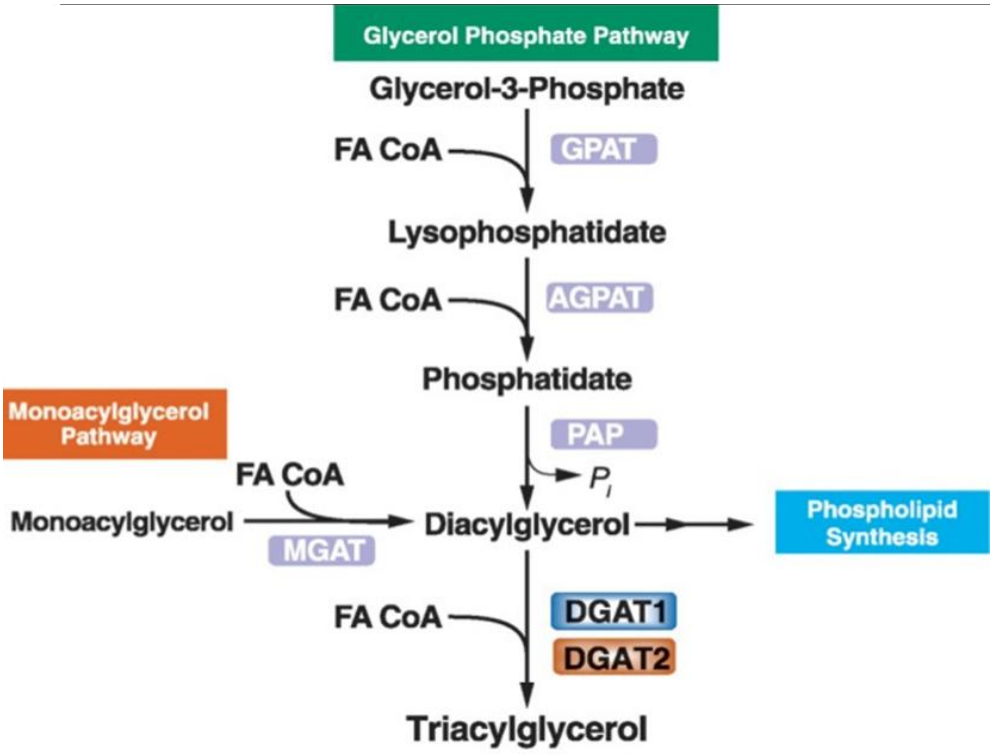

Figure4. Triacylglycerol synthesis and acyl-CoA:diacylglycerol acyltransferase (DGAT) enzymes. Triacylglycerols (triglycerides) are the end-product of a multi-step pathway. (Source: Yen et al., 2008)

In most insects, the fat body produces and secretes large amounts of DG leading to high hemolymph concentrations of this lipid [37]. This is a distinction between insects and vertebrates. MGATs and DGATs catalyze two consecutive steps of enzyme reactions in the synthesis of triacylglycerols (TAGs)[38]. The production of DG is dependent on the activities of both MGAT, produces DG, and DGAT, consumes DG. DG synthesis from MG and acyl-CoA is catalyzed by MGAT. Subsequent acylation of DG in a reaction catalyzed by diacylglycerol transferase, DGAT, produces TG. The genes of MGAT and DGAT in insects are of great importance, yet the detail still need to be explored.

Since the fat body is at the center of material storage and intermediary metabolism in insects, it plays a crucial role in the metabolism of pesticides [40]. Understanding lipid metabolism in fat body is also important to understand insect physiology and eventually find new ways to control the population of insects that negatively affect the production of crops or that act as vectors of human diseases. In such a context, we have pursued studies to further characterize three important enzymes of lipid metabolism: the triacylglyceride lipase in the triacylglyceride lipolysis pathway and the MGATs and DGAT of *Manduca Sexta.*

CHAPTER II

TGL-mediated lipolysis in *Manduca sexta* fat body: Possible roles for lipoamide-dehydrogenase (LipDH) and high-density lipophorin (HDLp)

1.Introduction

Lipolysis is a fundamental process at the center of energy metabolism. Insects accumulate TG as lipid droplets (LDs) within the cytoplasm of fat body cells during feeding periods, and then rely on these stores to support the energy requirements associated to non-feeding periods, sustained flight and embryo development [6]. TGs, the major lipid form, are stored in the core of the lipid droplets surrounded by phospholipids and a coat of proteins[41]. Lipid droplets are dynamic organelles whose metabolic role is dependent on the protein coat. Several of these proteins are involved in the regulation of triglyceride storage and mobilization[42].

Mobilization of TG stores from LDs is catalyzed by lipases. TGL is a major fat body lipase of Manduca sexta that is conserved among insects[43]. The most conserved regions of TGL coincide with the presence of functional domains: the WWE domain is located in the amino (N)-terminal part (residues 46–128), the lipase motif is in the central region (GHS367LG), and the DDHD domain is situated between residues 411 to 609 towards the C-terminal. The DDHD is a long domain commonly present in the proteins of the intracellular phospholipase A1 (iPLA1) family. A recent study showed that DDHD domain is essential for the enzymatic activity of mammalian iPLA1 [44]. Moreover, this domain also participates in the formation of homo-

oligomers through multiple interactions between the carboxyl (C)-terminal region containing the DDHD domain and the N-terminal half of mammalian iPLA1 .

The WWE domain, which is named after three of its conserved residues, has been identified in diverse cytosolic proteins with predicted ubiquitin- and ADP-ribosylation-related functions, and, in general, it is predicted to mediate protein–protein interactions[45]. WWE domain is most commonly found as a single copy motif but proteins of the Deltex family exhibit a tandem pair of WWE domains. Deltex proteins are cytosolic proteins of the Notch pathway that is involved in cell fate determination during several developmental processe[46]. In Drosophila, the WWE tandem modules localize at the N-terminal region of Deltex. Each module forms an autonomous fold in which the N and C termini within the module are in close proximity. Interactions between these two WWE modules create a compact and functional N-term domain by which Deltex interacts with the Notch receptor displaying its activity as modulator of the Notch pathway[46]. The function of WWE domain in TGL or any other lipase remains to be elucidated.

TGL localizes in the cytosol and is able to hydrolyze TG, DG, and phospholipids[9, 12]. Our understanding of how TGL activity is regulated is very limited. In vivo, TGL is constitutively phosphorylated, and the level of phosphorylation remains constant when lipolysis is stimulated by adipokinetic hormone [47]. The cAMP-dependent kinase, PKA, is involved in the activation of the lipolytic response induced by AKH[48]. PKA can phosphorylate TGL in vitro but the lipase activity remains unchanged after phosphorylation[13]. On the other hand, AKH provokes a rapid phosphorylation of Lsd1, a lipid droplet-associated protein, and this event results in the activation of TGL[49]. Phosphorylation of the lipid droplet accounts for about 70% of the AKH-induced lipolytic response[13].

In addition to the effect on the lipid droplets, AKH also induces lipase activation in the cytosol[50, 51]. In Manduca this effect accounts for the remaining 30% of the lipolytic response to AKH. The mechanism of this component of the lipase activation that, as mentioned above, is independent of changes in the phosphorylation state of TGL, remains unknown.

To better understand the mechanisms of regulation of TGL, we tried to identify potential TGL interacting proteins mediated by WWE domain using an in vitro system. By identifying these proteins, the key of the TGL regulation might be revealed and other functions of the TGL could also be infered by correlation with interesting candicates. Then we Investigated possible effects of the TGL interacting proteins on the activity of TGL.

2.Experiment Procedures

Materials

pET32 Ek/LIC vector, Escherichia coli strains Nova Blue and Rosetta 2, were obtained from Novagen (Billerica, MA). Ni-sepharose resin, PD-10 columns, and ECL chemiluminescence reagents were obtained from GE-Healthcare (Pittsburgh, PA). Protein A-Agarose (pre-blocked with albumin) was obtained from Santa Cruz Biotechnology (Dallas, TX). Glutathione [52], glutathione disulfide (GSSG), N-ethlymaleimide (NEM), Triton X-100, benzamidine, carmustine and auranofin were obtained from Sigma–Aldrich (St. Louis, MO). Dithiothreitol (DTT) and liquid scintillation counting cocktail were obtained from RPI (Mount Prospect, IL).M. sexta adipokinetic hormone [47] was obtained from Peninsula Laboratories (Belmont, CA). [Tri-9,10-3H]-oleoylglycerol was purchased from Perkin Elmer Life Sciences (Boston, MA). Precast 4–20% acrylamide gradient gels and BenchMark™ Protein Ladder containing proteins

with molecular masses of 220, 160, 120, 100, 90, 80, 70, 60, 50, 40, 30, 25, 20, 15, and 10 kDa were purchased from Invitrogen (Carlsbad, CA). Pre-cast 4–15% acrylamide gels were purchased from Bio-Rad (Hercules, CA). DNA sequencing was performed by the Core Facility of our department using an ABI Model 3700 DNA Analyzer. All other chemicals were of analytical grade.

2.1. Insects

M. sexta eggs were purchased from Carolina Biological (Burlington, NC), and larvae were reared at 25 °C on an artificial diet. Adult insects were maintained at room temperature without food. Fat bodies from adult male insects (second day after emergence) were placed in liquid nitrogen immediately after dissection and stored at −80 °C.

2.2. Cloning, expression and purification of N terminus region containing WWE domain

The N-terminal region of the M. sexta TGL gene (encoding amino acids 1–140) was amplified by polymerase chain reaction (PCR) using the following forward and reverse primers: 5′-GACGACGACAAGATGAACGATAGTACGGAAAGGA-3′ and 5′-GAGGAGAAGCCCGGTCTATCTGGCGTCAGTGGGACCT-TTG-3′, respectively, and a plasmid containing full-length Manduca TGL cDNA (pGEM-TGL) that was previously prepared[43]. The amplified product was ligated into pET32 Ek/LIC vector as previously reported[49], and the sequence of the recombinant plasmid was confirmed by DNA sequencing. The N-term region of TGL was expressed as a recombinant fusion protein containing thioredoxin, poly-His and S-tag (Trx-[His]6-Stag-WWE). Expression of the fusion protein was induced with

1 mM IPTG for 3 h. For the preparation of cell extracts, the bacterial pellet was resuspended in buffer (50 mM Tris pH8, 1 mM EDTA, 100 mM NaCl, 1 mM PMSF) containing 0.3 mg/ml of lysozyme. After 30 min incubation, the preparation was centrifuged at 20,000g for 1 h. The fusion protein was found in the pellet, which was resuspended in 20 mM Tris buffer pH 7.9 containing 6 M urea. The supernatant was collected after centrifugation (20,000g for 30 min) and loaded into a Ni-affinity column. Proteins were eluted by increasing concentrations of imidazole (20–200 mM) in the same buffer. The fusion protein (Trx-WWE) was eluted with 200 mM imidazole. The purified protein was dialyzed against 10 mM Tris buffer pH 7.9 containing 250 mM NaCl, and subsequently treated with enterokinase to remove Trx and the poly-His/S-tag. After incubation, the sample was passed through a small column of Ni-Sepharose and the N-terminal region containing the WWE domain (amino acids 1–140) was recovered in the flow through. The WWE domain was dialyzed against 50 mM phosphate buffer, pH 7.4 and analyzed by SDS-PAGE and circular dichroism.

2.3. Circular dichroism (CD)

CD spectroscopy was carried out in a Jasco-715 (Jasco Corporation, Tokyo, Japan) spectropolarimeter. Quadruplicates of the spectra were averaged, corrected for background, and smoothed and the mean residue ellipticity (deg cm2 dmol−1) was calculated. The secondary structure of the recombinant WWE domain was estimated with the program DichroWeb[53].

2.4. WWE interacting proteins assay

Immobilization of Fusion Protein in Ni-Sepharose beads: Trx-WWE (840 μg) was bound to Ni-sepharose beads (500 mg) and washed with PBS (1 mM KH2PO4, 3 mM Na2HPO4, 155 mM

NaCl; pH 7.4). The resin (Trx-WWE-Ni) was split into two identical fractions of 250 mg, which from now on, were handled in parallel. In one fraction, the lipase domain was removed by proteolytic cleavage with thrombin followed by one step wash with PBS to generate Trx-Ni ("control" resin). The other half of the resin (Trx-WWE-Ni) was subjected to the same procedures as "control" resin but thrombin was omitted in the buffer. All steps were carried out on ice or at 4 °C. Fat body soluble proteins: two fat bodies were homogenized in 2 ml of PBS containing 1 mg/l aprotinin and 1 mM PMSF. Infranatant was collected after centrifugation (20,000g for 30 min), and protein concentration adjusted to 20 mg/ml. Assay: 150 µl of fat body soluble proteins were incubated with each type of resin for 2hr and subsequently washed four times with 1 ml PBS. Proteins were eluted in one step by incubation with 150 µl of 1 M imidazole. Aliquots of the eluted proteins were subjected to SDS-PAGE (4–20% gradient gels) and analyzed further by mass spectrometry and western blotting. Data were collected from two independent experiments.

2.5. Protein identification by mass spectrometry

Each lane of the Coomassie Blue stained gel was sliced in six regions. During all the steps control and test samples were treated in exactly the same way. Each slice was minced and proteins were prepared for trypsin digestion as previously reported[54]. Digestion products were analyzed by LC-MS/MS on a hybrid LTQ-Orbitrap XL mass spectrometer (Thermo Fisher Scientific) coupled to a New Objectives PV-550 nanoelectrospray ion source and an Eksigent NanoLC-2D chromatography system. Other technical details and the methods used for peptide and protein identification were done as described previously[54].

2.6. Western blotting

Proteins were separated by SDS-PAGE on 4–20% (Invitrogen) or 4–15% (Bio-Rad) acrylamide gels. The gels were blotted onto nitrocellulose membranes using a wet system from Invitrogen or the Trans-Blot Turbo system from Bio-Rad and further incubated with rabbit polyclonal antibody specific for TGL that was raised using recombinant N-terminal region (amino acids 1–140) by Cocalico Biologicals (Reamstown, PA), apolipophorin I/II that was raised in rabbits using purified HDLp from the hemolymph of larval insects by Cocalico Biologicals (Reamstown, PA). The following commercial antibodies that were raised in rabbits were also used: glutathione S-transferase I (Abcam, Cambridge, MA), lipoamide-dehydrogenase (Abcam, Cambridge, MA), Stag (Novagen, Billerica, MA) and lipoyted proteins (Calbiochem, Billerica, MA). After incubation of the blots with horseradish peroxidase-conjugated anti-rabbit secondary antibodies (Santa Cruz Biotechnology, Dallas, TX), the immunocomplexes were detected by enhanced chemiluminescence (ECL GE Healthcare).

2.7. Subcellular fractionation of fat body

Fat body tissue from two male adult insects were dissected, thoroughly washed, pooled and immediately homogenized with a Potter-Elvehjem glass homogenizer fitted with a Teflon pestle, using 3 ml of HB buffer (50 mM Tris, pH 7.4, 1 mM EDTA, 250 mM sucrose, 0.1 mM benzamidine, 10 mM DTT, 1 mM PMSF). The homogenate was centrifuged to 1000g for 10 min. The resulting soluble fraction was centrifuged at 20,000g for 30 min. The pellet was collected and the supernatant of 20,000g (SN20) was overlaid with 1 ml buffer PBS and centrifuged at 100,000g for 1 h. Three fractions were collected: fat cake, infranatant (cytosol) and pellet (P100). Both pellets (P20 and P100) were resuspended in 3 ml PBS and re-centrifuged. Both pellets were resuspended 1 ml of buffer and centrifuged at 500g for 15 min. The resulting supernatant was

used as membranes fraction (P20 and P100, respectively). Fat cake containing the lipid droplets were collected from the top and resuspended in 0.5 ml PBS. Protein concentration was determined in all fractions and samples were analyzed by western blotting for LipDH and HDLp.

2.8. Lipase activity

Four fat bodies were combined with 3 ml of HB buffer (50 mM Tris, pH 7.4, 1 mM EDTA, 250 mM sucrose, 1 mM benzamidine, 10 mg/l leupeptin, 1 mg/l aprotinin) and homogenized. All steps were carried out on ice or at 4 °C. The homogenate was overlaid with 1 ml of buffer without sucrose, and subjected to centrifugation at 20,000g for 30 min. The infranatant (soluble fraction) was collected and total protein was determined. Aliquots of the soluble fraction of fat body containing 150–200 μg total protein were used to measure the lipase activity that was assayed with a micellar TG substrate containing [3H]-TG and Triton-X-100 as previously described[8]. The assay mixture (0.1 ml) contained 50 mM Tris, 500 mM NaCl, 0.05% (v/v) Triton X-100, 0.25 mM triolein [0.002 Ci/mmol], pH 7.9. To determine the effect of carmustine (75–560 μM) and auranofin (1 and 75 μM) on lipase activity, samples were pre-incubated with increasing concentrations of inhibitors for 30 min on ice. Control assays were carried out in the absence of inhibitors. Lipase activity was measured in the absence and presence of 10 mM DTT in triplicate reactions in a total of three independent experiments. Lipase activity was expressed as fold change over control (no inhibitor).

2.9. Triglyceride-lipase thiol groups

TGL was partially purified from the cytosolic fraction of M. sexta fat body homogenates using anion-exchange, hydroxyl-apatite, and hydrophobic interaction chromatography as reported

previously[9]. To determine the effect of DTT, GSH, and GSSG on the lipase activity, 15 µg of partially purified TGL was pre-incubated for 30 min on ice with increasing concentrations (0, 3, 6 and 12 mM) of each reagent followed by lipase activity assay that was carried out as described above. To determine the effect of N-ethlymaleimide (NEM), 1–6 µl (or nothing in the control sample) of NEM (500 mM in ethanol) were added to 80 µl of lipase preparation (0.75 µg/µl) that was previously treated with 10 mM DTT. The final volume was 100 µl, and the amount of ethanol was adjusted to be the same in all samples. After 30 min incubation on ice, lipase activity was determined as indicated above. Lipase activity was expressed as fold change over control (no addition).

2.10. Effect of AKH on lipase activity

Adult insects were decapitated for 24hr and injected with 13 mg trehalose. After 2 h, 100 pmol of AKH were injected and fat body tissue was dissected 20 min after the hormonal injection. Control group was injected with PBS. Freshly prepared fat bodies from two insects were pooled, homogenized and centrifuged as described above (Section 2.8). Lipase activity in soluble fraction was immediately assayed in the absence and presence of 10 mM DTT (Section 2.8). Lipase activity was expressed as nmol TG/mg protein min.

2.11. Co-immunoprecipitation

Fat body soluble proteins (50 µl having approximately 500 µg total protein) was combined with 2 µl of rabbit anti-HDLp antibody for 2 h at 4 °C, followed by addition of 20 µl of Protein-A-Agarose beads and incubated overnight. After centrifugation (1000g for 5 min), the pellet was washed four times with 1 ml PBS. The resulting immunoprecipitates were resuspended in

Laemmli sample buffer, and proteins were subjected to SDS-PAGE (4–15% gradient gels) to be analyzed further by mass spectrometry and western blotting.

2.12. Intracellular distribution of HDLp, TG and DG

Sucrose density centrifugation: freshly dissected adult fat bodies were homogenized as indicated above using 3 ml of HB Buffer. The homogenate was centrifuged at 1000g for 10 min and the resulting supernatant was adjusted to 50% sucrose and transferred to an SW40 centrifuge tube to be subsequently overlaid with 1.0 ml each of 40%, 35%, 20%, 10%, 5% in HB buffer plus an additional layer of 1.5 ml of PBS. The tube was centrifuged at 160,000g for 4 h. The gradient was fractionated into seven fractions and each fraction analyzed to determine protein, apoLp I/II, DG and TG. Proteins were separated by 4–15% SDS-PAGE. For the top six fractions the gels were loaded with 0.6% of each fraction. For the cytosolic fraction 0.1% of the fraction was loaded in the gel. The separated proteins were transferred to nitrocellulose membranes and subjected to western blotting using anti-HDLp antibody. The proportions of DG and TG were determined by thin layer chromatography (TLC) of lipid extracts. To this end, lipids from aliquots of the gradient fractions were extracted with chloroform: methanol (2:1 v/v) and separated by TLC in hexane/ethyl ether/formic acid (70:30:3 v/v/v). MG, DG, FA and TG spots were visualized using iodine vapor, scanned and quantified with AlphaEaseFCTM software. TG and DG contents were expressed as percentage of total neutral lipid.

2.13. Lipophorin purification

Hemolymph from adult insects was collected in the presence of 30 mM KH_2PO_4, 2 mM EDTA and 10 mM DTT. Hemolymph was centrifuged at 4 °C for 15 min at 4500g. The supernatant was

adjusted to 0.5 g/ml KBr and overlaid with PBS containing 0.1 g/ml KBr. The sample was centrifuged at 340,000g in the Beckman rotor VTi65.2 at 10 °C for 1 h. The density gradient was fractionated from top to bottom, and the fractions containing HDLp were collected (fractions 3 and 4). After desalting the fractions by gel filtration, the purity of HDLp was assessed by SDS-PAGE, and the protein concentration was determined.

2.14. Effect of HDLp on TGL activity

The activity of partially purified TGL was assayed in the presence of HDLp or albumin (BSA) as control. The assay mixture (0.1 ml) contained 50 mM Tris, pH 7.9, 25nomles of [9,10-3H]-triolein, 0.002 Ci/mmol, 0.05% (v/v) Triton X-100, 500 mM NaCl, 10 mM DTT and the corresponding amount of HDLp or BSA (0–5 μg). The reaction was started by adding TGL (15 μg) and incubated at 37 °C with constant shaking for 30 min. Blank reactions did not contain lipase. The reaction was stopped by adding 500 μl of CHCl3/methanol/benzene (2:2.4:1 vol.) and 40 μl 1 N HCl. The organic phase was obtained, dried, and separated by TLC. Spots corresponding to each lipid form were scraped. Silica was transferred to a vial containing 4 ml of scintillation cocktail and the radioactivity determined by liquid scintillation counting to determine the hydrolysis products as previously described. Results were expressed as nmoles of lipid produced (DG, MG) and consumed [5] per reaction. Values represent the mean ± SEM of three determinations.

2.15. Other methods

SDS-PAGE was performed according to Laemmli and proteins were visualized by Coomassie

Brilliant Blue R staining. Protein concentrations were determined by the Bradford dye-binding assay using bovine serum albumin (BSA) as standard. Data were presented as the mean ± SEM. Statistical comparisons were made by one way ANOVA with post test.

3.Results and Discussion

3.1. Identification of TGL interacting proteins

The WWE domain is a 90-amino acids fragment situated between amino acids 40 to 128 of Manduca TGL[43]. The function of this domain in TGL is unknown. A significant sequence alignment between amino acid 40 and 140 of TGL and the second WWE domain of Drosophila Deltex, for which the structural information is available, was found. Fig. 5A shows the alignment of Manduca and Drosophila WWE sequence motif, and the three conserved residues – two tryptophans and glutamic acid – characteristic of WWE domain are indicated. We cloned the cDNA encoding amino acids 1–140 of TGL, and the recombinant protein was overexpressed in E. coli as a fusion protein with thioredoxin, polyHis and Stag (Trx-[His]6-Stag-WWE). The expression of the fusion protein was confirmed by western blot using Stag antibodies (not shown). Purified fusion protein was cleaved with enterokinase to remove the fusion tags (Fig. 5B), and the secondary structure of resulting protein (WWE) was analyzed by circular dichroism (CD) (Fig. 5C). Deconvolution of the CD spectrum indicated that the N-term region was folded. The estimated proportions of α-helix, β-strands, turns, and unordered structures were 22.5%, 22.4%, 21.7% and 33.4%, respectively. This structural composition is compatible with the fold of Deltex WWE domains deduced from the crystal structure[46].

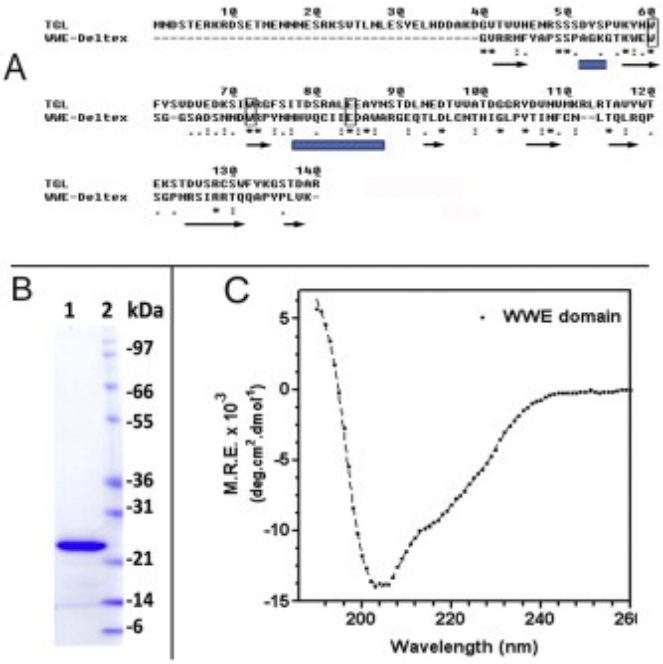

Fig 5. Sequence, Expression and Circular Dichroism of N-terminal region of TGL. A) The amino acid sequence alignment of the N-terminal region of MsTGL with Drosophila WWE-Deltex sequence is shown. The sequence alignment was generated using Alignment Explorer/Muscle (Edgar, 2004). Identical residues in the sequences are denoted by asterisks; conservative substitutions are denoted by dots. The locations of α-helices (rectangles) and β-strands (arrows) identified from the crystal structure of WWE-Deltex were adapted from[46]; B) Coomassie Blue stained SDS-PAGE of the purified 140-residue polypeptide, which was expressed as a fusion protein with thioredoxin, cleaved with enterokinase and then purified; C) Far-UV CD spectrum of the purified N-terminal domain of TGL [amino acids 1–140].

Recombinant TGL N-term proved to be a stable polypeptide having the predicted fold, and we

utilized this protein to search for TGL interacting proteins. Fusion protein, Trx-[His]6-Stag-WWE, was immobilized to Ni-sepharose beads and incubated with the soluble fraction of fat body homogenate. As a control, an identical assay was carried out in parallel using resin in which only the tag portion of the fusion protein (Trx-[His]6) was bound. After multiple washes, proteins were eluted with imidazole and analyzed by SDS-PAGE coupled to mass spectrometry (MS/MS). Fig. 5A shows a representative acrylamide gel with the protein profiles for test (lane 1) and control (lane 2) resin. The fusion protein (MW = 33.3 kDa) and control protein (MW = 13.9 kDa) can be seen as major bands of lanes 1 and 2, respectively, together with co-eluted proteins. Each gel line was sliced in sections that were analyzed by MS/MS as indicated in Methods. A comparison of the levels of spectral counts was used to distinguish the proteins that were more abundant in the test samples. A threshold of 1.5-fold increase in the test sample over control was chosen to minimize potential artifacts.Table 1 shows the list of proteins that matched this criterion in two independent experiments. A total of thirteen proteins were identified. Antibodies were available for four of these proteins (apolipophorin precursor – apoLp-I/II-, LipDH, glutathione S-transferase and TGL). Western blotting analyses of the eluate from control and test resins confirmed the enrichment detected by MS/MS (Fig. 6B). In addition, to confirm the interaction of TGL and apoLp-I/II we carried out immunoprecipitation using anti-HDLp antibodies. The immunoprecipitates were analyzed by MS/MS and western blotting using anti-TGL antibodies. TGL was detected in the immunocomplex confirming that TGL binds HDLp (Fig. 7). In addition to TGL, four other proteins were also identified in the immunocomplex by MS/MS. These proteins are indicated in Table 1.

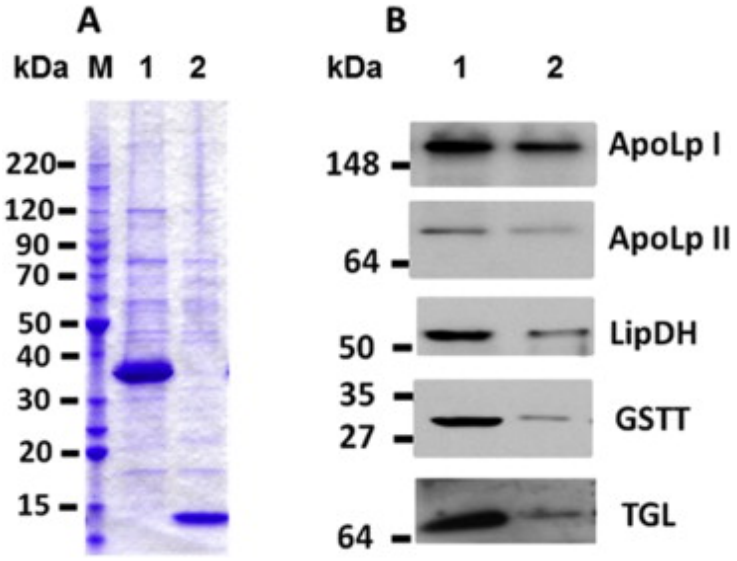

Fig6. WWE Interacting Proteins Assay. A) Coomassie blue stained gel of the soluble proteins eluted from by Ni-sepharose beads containing Trx-WWE fusion protein (lane 1) or Trx (lane 2). Fat body soluble proteins were incubated with 12.5 nmol of Trx-WWE bound to Ni-sepharose beads for 2 h and the resin was subsequently washed four times with buffer. Proteins were eluted in one step by incubation with 1 M imidazole. Co-eluted proteins were analyzed by SDS-PAGE in 4–20% acrylamide gradient gels (lane 1). Control experiment was carried out using 12.5 nmol of Trx bound to Ni-sepharose beads (lane 2). Protein markers (BenchMark protein ladder) are shown in lane M (see Materials). B) Western blotting: aliquots of eluted proteins from test (lane 1) and control (lane 2) resins were separated by SDS-PAGE in 4–20% acrylamide gel and transferred to nitrocellulose. Blots were analyzed by immunodetection for the following proteins: ApoLp-I and II, LipDH, GST and TGL as indicated in Materials and Methods. (For interpretation of the references to color in this figure legend, the reader is referred to the web version of this article.)

Identified protein	Accession number	Spectral counts (SC)		SC ratio
		Trx-Wwe	Trx	
1 – Apolipophorin precursora	2498144	88	19	4.6
2 – Arylphorin subunit betaa	1168527	77	3	25
3 – Trehalose 6-phosphate synthasea	281372519	71	48	1.5
4 – Dihydrolipoamide dehydrogenase	6014978	67	39	1.7
5 – Pyruvate-kinase	259450896	53	29	1.8
6 – V-type proton ATPse subunit H	12585497	53	32	1.7
7 – Transketolasea	114050833	43	21	2.0
8 – Glutamate dehydrogenase	114052462	31	15	2.0
9 – Kinesin-like protein 1	309378082	27	5	5
10 – Glutathione S-transferase theta	170779021	22	15	1.5
11 – V-type proton ATPase subunit D	12585494	20	6	3.3
12 – Tubulin beta-1 chaina	121987496	18	5	3.6
13 – Triglyceride-lipasea	238846408	70	11	6.4

Table 1.

WWE interacting proteins identified by MS/MS. The table shows the proteins that interact with the WWE domain. The list includes proteins whose spectral counts (SC) were at least

1.5-fold greater in the test (Trx-WWE) resin than in the control resin (Trx), in two experiments. The SC and the SC ratio between the samples eluted from test and control resins observed in one of the experiments are shown. In bold are the proteins in which antibody was available and MS/MS results were confirmed by Western blot.

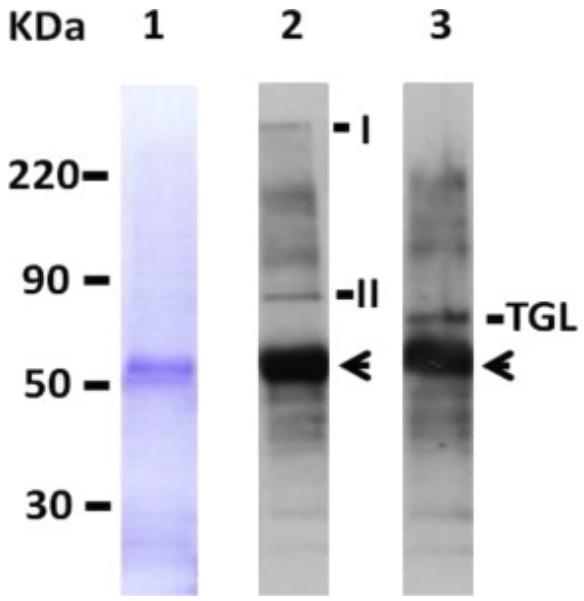

Fig 7. Co-immunoprecipitation of TGL with anti-HDLp antibodies. Fat body soluble proteins were incubated with anti-HDLp antibody for 2 h and immunoprecipitated using protein-A-agarose beads preblocked with BSA. After washing the beads four times with PBS the associated-proteins were separated by SDS-PAGE gel in 4–15% acrylamide gel (lane 1), and analyzed by western blotting using anti-HDLp (lane 2) and anti-TGL antibodies (lane 3). The arrow indicates IgG. ApoLp I/II and TGL bands are also shown in lane 2 and 3, respectively.

Several of the proteins shown in Table 1 are enzymes including TGL. The presence of TGL indicates that the lipase is able to form homodimers. Dimers could be maintained through WWE–WWE interactions such as occurs in proteins of the Deltex family[46]. However, the large DDHD domain present in the C-term of TGL could also interact with the N-term region of a second TGL molecule, as recently reported in the homodimer formation of vertebrate phospholipase iPLA1 [44].

Three of the TGL interacting proteins – transketolase, trehalose synthase and pyruvate kinase – are central enzymes of carbohydrate metabolism. Transketolase connects the pentose pathway and glycolysis whereas trehalose synthase catalyzes the synthesis of trehalose. Pyruvate kinase catalyzes the last step of glycolysis where pyruvate and ATP are produced. Pyruvate kinase and trehalose synthase are linked in the sense that both compete for glucose. The glycolytic pathway has to be inhibited for trehalose synthesis to occur. Interestingly, ATP is an inhibitor of both TGL[8] and vertebrates' pyruvate kinase. Moreover, glutamate dehydrogenase (GDH), a TGL interacting protein (Table 1), is also inhibited by ATP in mammals. GDH catalyzes the oxidative deamination of glutamate raising the cellular content of NAD(P)H. Lipoamide dehydrogenase (LipDH) was also identified as TGL interacting protein (Table 1). This enzyme catalyzes a reversible reaction in which NADH is a substrate. Despite the fact that all the proteins identified in Table 1 belong to different metabolic pathways, yet a certain connection can be recognized. One would think that the regulation of the activity of these enzymes that have substrates or products in common would be enhanced if they are in close proximity as these results are suggesting. Likewise, the transfer of NADH from one enzyme to another would be facilitated if the enzymes are in a complex.

Glutathione S-transferase (GST) was also identified in Table 1. GSTs are cytosolic enzymes that

catalyze the conjugation of glutathione to a wide range of substrates including the product of lipid peroxidation that are toxic for the cell. Two subunits of the V-type proton ATPase, a multimeric enzyme involved in ATP-dependent acidification processes related to vesicular transport including endocytosis and exocytosis, in addition to the structural components of high density lipophorin (HDLp), and some elements of cytoskeletal structure (kinesin-like protein and tubulin b) were also identified as TGL interacting proteins.

We have demonstrated that the N-terminal region of TGL forms a protein fold compatible with that of the WWE domain. Furthermore, this region was able to mediate protein–protein interactions corroborating the predicted functionality of the WWE domain. The data suggest that TGL occurs as a multi-protein complex mediated in part by interactions through the WWE domain. In addition to the possibility of forming homodimers, TGL interacts with other enzymes of intermediary metabolism including redox-active proteins, lipid transport proteins (HDLp lipophorin), and proteins of the cytoskeleton. The physiological connection between TGL and these proteins is unknown. In this study we focused on two of these proteins: LipDH, and apoLp I/II, the apolipoprotein component of HDLp, the main carrier of diacylglycerol in the hemolymph. Further studies were undertaken to try to understand the implications of the interaction between TGL and each of these proteins.

3.2. TGL-LipDH interaction

LipDH (EC 1.8.1.4) is a conserved protein best known as an integral component of mitochondrial α-keto acid dehydrogenase complexes. In rat liver 90% of the enzyme localizes in the mitochondria[55]. It catalyzes the oxidation of the dihydrolipoyl cofactor of the acyltransferase (E2) component of the multienzymatic complexes with NAD+ as the electron acceptor. M. sexta LipDH has been cloned and sequenced[56]. The predicted protein has an

estimated mass of 51 kDa and is a relatively well conserved protein[56]. Preliminary immunoblot studies showed that the protein can be detected in the fat body using antibodies raised against LipDH isolated from porcine heart. First we studied the subcellular distribution of LipDH in the fat body of M. sexta adult insects by differential centrifugation and western blotting. We discovered the presence of LipDH in all subcellular fractions including cytosol, fat cake and membranes (Fig 8). Taking into account the distribution of total protein among subcellular fractions, it was estimated that 65 ± 14% of total cellular LipDH localizes to the cytosol whereas 34 ± 14% localized to the fractions containing membranes (mitochondria, plasma membrane, microsomes, and lipid droplets). To our knowledge the high levels of cytosolic LipDH represents a new finding in animals. The presence of LipDH outside the mitochondrial complexes has been reported in trypanosomes and archaebacteria so far. In these species LipDH is found associated to the plasma membrane[57, 58] and the cytosolic fraction[59]. No physiological substrate for these forms of the enzyme in those organisms has been reported.

Fig 8. Subcellular Localization of LipDH in M. sexta Fat Body. Subcellular fractions of adult fat body homogenates were separated by SDS-PAGE and analyzed by western blotting using anti-LipDH antibody. Approximately 10 µg (lanes "a" and "d") and 30 µg (lanes "b" and "c") of total proteins were loaded in the corresponding lane. Lane a: lipid droplets; lane b: cytosol; lane c: 100,000g pellet (P100); lane d: 20,000g pellet (P20). A representative western blotting result is shown.

The function of LipDH is to catalyze the oxidation of dihydrolipoyl covalently attached to protein.

Next we examined whether recombinant fusion protein has lipoate as a cofactor. Western blotting using antibody specific for lipoylated proteins revealed a very strong response suggesting the presence of a lipoyl residue in the fusion protein (data not shown). Next we analyzed the protein by MS/MS to identify lipoylated peptides. However, MS/MS analyses failed to identify any lipoylation site in the fusion protein despite that all peptides were accounted (100% sequence coverage). No peptide showing a lipoyl modification was detected by MS/MS after triplicate analyses using protein samples obtained from independent preparations including a sample in which recombinant protein was expressed in a culture supplemented with lipoic acid. The robust response in the western analyses using antibodies specific for protein-bound lipoic acid suggested a high level of lipoylation in the N-term region of TGL. Although MS/MS result cannot exclude lipoylation in a small fraction of the protein, it indicates that the vast majority of protein did not contain lipoic acid as cofactor. Lipoylation is a post-translational modification in which lipoate is attached via amide linkage to the amino group of the side chain of a specific lysine residue of the target protein. Several lysine residues are present in the N-term region of the lipase but the conserved lipoyl attachment domain (PF00364) that is identified in lipoylated proteins is not found in TGL.

LipDH is a member of the pyridine nucleotide-disulfide oxidoreductase family that includes glutathione reductase (GR) and thioredoxin reductase, TrxR. The last two enzymes catalyze the NADPH-dependent reduction of oxidized glutathione (disulfide glutathione) and thioredoxin, respectively. In vertebrates, GR and TrxR have a prevalent role in the balance of cellular redox homoeostasis[60]. However, Drosophila lacks GR and its function is substituted by TrxR[61]. Inspection of the available genomes suggests that this could be a general case in insects. LipDH catalyzes the electron transfer between pyridine nucleotides and disulphide compounds such as

lipoic acid and the reaction is reversible[62]. The presence of LipDH in the cytosol could be needed to substitute for the absence of GR and maintain the redox state of cytosol. The disulfide-oxidoreductase activity of cytosolic LipDH could also serve to keep the thiol groups of TGL in a reduced state. TGL exhibits four strictly conserved Cys[43]. Cys 130 and Cys 234 are flanking the predicted lid region of TGL[43]. The lid, which is present in lipases of the α/β hydrolase family, covers the active site, and rotates allowing the interaction with the substrate. The flanking Cys are thought to be involved in the mechanism of lipase activation. To verify the occurrence of thiol groups in TGL that are essential for its activity, we measured the activity of purified TGL in the presence of increasing concentrations of reduced [52] and oxidized glutathione (GSSG) and DTT. As shown in Fig. 9A, the activity gradually increased in the presence of reducing agents – DTT and GSH – doubling its value at 12 mM. In contrast, the incubation with 12 mM GSSG decreased the lipase activity to ~50% of the activity control. The inhibitory effect of GSSG could be explained by the formation of mixed disulfide or glutathionylation between the GSSG and

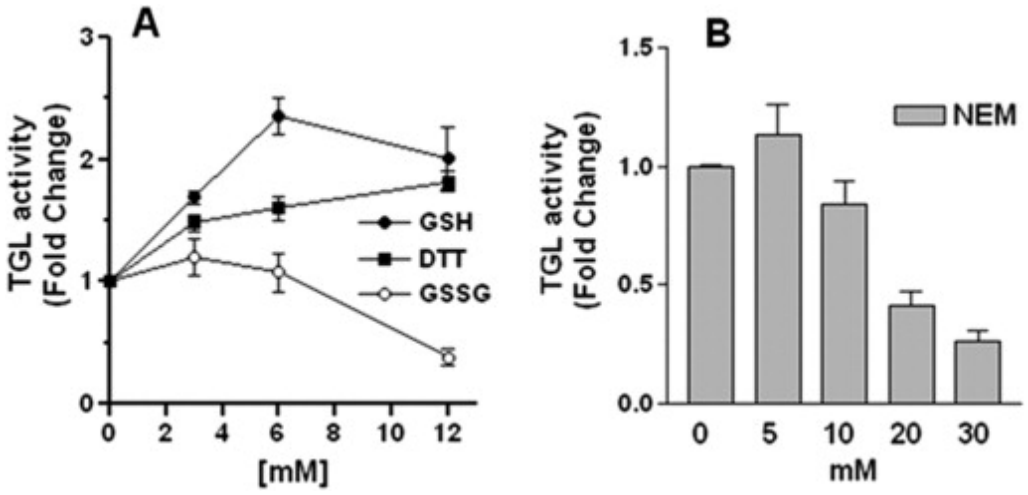

Fig 9. Effect of DTT, GSH, GSSG and NEM on TGL Activity. Partially purified TGL was pre-incubated with the indicated concentrations of DTT, GSH, GSSG (A), NEM (B) for 30 min on ice prior to measure the lipase activity. Lipase activity was expressed as a fold change relative to control (no addition). Values are the mean ± SEM of three independents experiments.

reactive lipase thiol groups as being described for other proteins such as isocitrate dehydrogenase[63, 64]. Furthermore, alkylation of thiol groups with NEM also showed a deleterious effect on the activity of TGL (Fig. 9B). These results indicate that TGL activity is sensitive to the redox status of the environment. The enzyme activity is preserved when the redox-sensitive thiol groups of the lipase are in the reduced-state.

3.2.1. Effect of carmustine and auranofin on lipase activity

Carmustine[65] and Cd+2 are LipDH inhibitors. Next we tested the effect of carmustine on the lipase activity of fat body homogenates. Carmustine was assayed at concentrations ranging between 75 to 560 μM and showed a significant inhibitory effect on the lipase activity starting at 75 μM (Fig 10A). In contrast, carmustine did not affect the activity of purified TGL even at 1.5 mM (not shown). Therefore the inhibitory effect of carmustine on the lipase activity of fat body homogenates could be interpreted as an indirect effect due to the inhibition of LipDH. Carmustine has been originally described as a LipDH and GR inhibitor[65]. However, carmustine can also act on TrxR at concentrations ranging from 0.1 to 1 mM[66]. To investigate whether the effect of carmustine on the lipase activity was due TrxR inhibition rather than LipDH, we tested the effect of auranofin, which is a very potent inhibitor of TrxR that is effective at nanomolar

range, whereas 1000-fold higher concentrations inhibit GR[67]. The effect of auranofin was tested in a range of concentrations between 1 and 75 μM. We chose this range because it was shown that 1 μM auranofin efficiently inhibited (90%) Drosophila TrxR. However, no significant inhibition on the lipase activity was observed at concentrations ranging from 1 to 10 μM. The inhibitory effect of auranofin on the lipase activity was observed at the concentration range in which auranofin inhibits GR and LipDH (25 μM) (Fig. 10B). The inhibition in both cases was reversed by 10 mM DTT indicating that the action of these inhibitors indirectly impacted the redox state of thiol groups of lipase (Fig. 9A–B). Furthermore, LipDH inhibition by carmustine caused a greater lipase inhibition than the inhibition of thioredoxin reductase (1–10 μM range) by auranofin. Taken together these results are consistent with the idea of LipDH playing a role in the control of the redox state of TGL critical thiol groups. In this way, LipDH would catalyze the reverse reaction acting as a disulfide reductase.

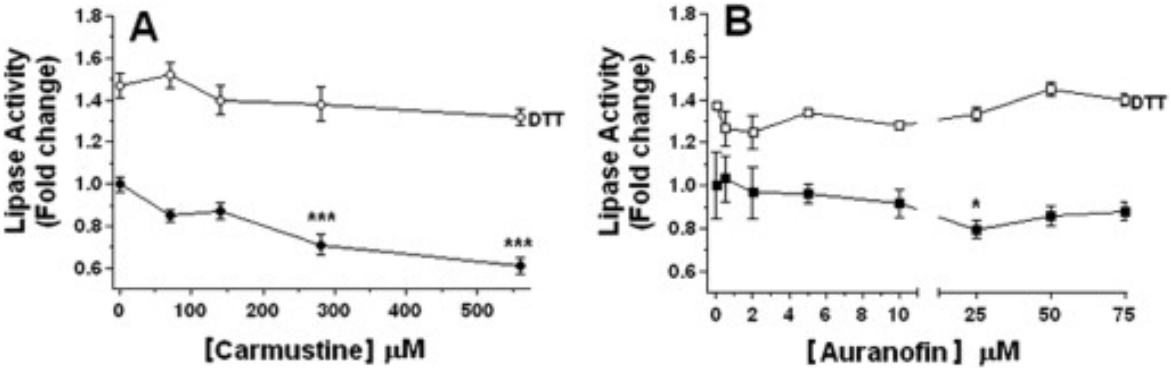

Fig 10. Effect of Carmustine (A) and Auranofin (B) on lipase activity. Fat body soluble fractions were pre-incubated with the indicated concentrations of inhibitor for 30 min on ice prior to measure lipase activity. Experiments were conducted in the presence and absence of 10 mM DTT. Lipase activity was expressed as a fold change relative to control (no inhibitor). Values are the mean ± SEM of three independent experiments. Significant

differences determined by one way ANOVA are shown with asterisks. [***] indicates p < 0.001 and [*] indicates p < 0.05.

As mentioned above, the physiological function of LipDH is to catalyze the oxidation of the dihydrolipoyl cofactor of the acyltransferase component of the multienzymatic complexes with NAD+ as the electron acceptor. However, in vitro, the enzyme can also act as a diaphorase and catalyzes the reverse reaction, in which the oxidation of NADH occurs. Some diaphorase substrates of LipDH are: NO[62], O2[68], lipoamide[62], cytochrome c, quinones[68], and methylene blue.

Manduca LipDH is more related to GR than TrxR. The mechanisms of LipDH and GR have been found to be very similar to each other in several organisms. LipDH could also compensate for the lack of GR and be involved in the metabolism of glutathione catalyzing the recycling of GSSG to GSH. Alternatively, cytosolic LipDH could catalyze the reduction of protein-dithiol-disulfide using reducing equivalents from NADH. Likewise, the enzyme could act on mixed disulphide bonds, such as those formed between GSH and protein-thiols under oxidative stress conditions to prevent further oxidation of the protein-thiols[60, 69]. Unlike the mammalian system in which only 10% of LipDH is extramitochondrial, in the fat body more than 50% of the enzyme localizes in the soluble fraction. A study on Bombyx mori LipDH showed that recombinant protein was a soluble enzyme able to catalyze the lipoamide-dependent oxidation of NADH[70]. Altogether this information suggests that LipDH plays an additional function in insects. According to this study, LipDH seems to be part of the antioxidative system of the cell in control of the redox status of protein-thiols, and its activity prevents lipase inactivation.

3.2.2. Effect of AKH on lipase activity in the presence and absence of reducing agents

Previous work in our laboratory has shown that TGL is a major cytosolic lipase, and AKH induces an increase in the lipase activity of cytosol. In addition, the activation is independent of the lipase phosphorylation state[70]. We asked whether the AKH-induced lipase activation could be due to a change in the redox state of critical thiols. In that case, AKH could shift the ratio between the oxidized (inactive) and reduced (active) thiol groups of TGL. In this scenario, it could be possible to observe a smaller change in lipase activity of AKH-treated cytosols when assayed in the absence of DTT compared to the activity of control cytosols measured in the presence of DTT. This possibility was examined by measuring the lipase activity of freshly prepared cytosols from control and AKH-treated insects in the presence and absence of 10 mM DTT. Results confirmed the increase in lipase activity induced by AKH as previously observed ($p_{bd} < 0.001$)[13]. However, the extent of the lipase activation observed in the absence of DTT (Fig 11, bar c) was lower than in the presence of DTT (Fig 10, bar d, $p_{cd} < 0.001$) and higher than the activity of control samples measured in the presence of DTT (Fig 10, bar b, $p_{bc} < 0.05$). Thus, these results imply that changes in the redox state of lipase thiol groups cannot account for the lipase activation that was observed in AKH-treated insects. The above results suggest that some other undefined mechanism is involved in the AKH-induced lipase activation.

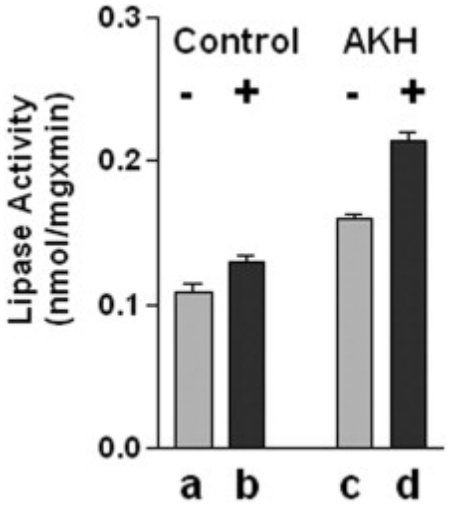

Fig 11. Effect of AKH on lipase activity in the presence and absence of reducing agents. Freshly dissected fat bodies from two insects that were injected with PBS (Control, bars a–b) or AKH (AKH, bars c–d) were pooled and homogenized. Fat body soluble fractions were tested for lipase activity in the absence (−) and presence (+) of 10 mM DTT. Lipase activity was expressed in nmol TG hydrolyzed/min.mg of total protein. Values are the mean ± SEM of three independents experiments. Pvalues are: pab > 0.05; pac < 0.001; pad < 0.001; pbc < 0.05; pbd < 0.001; pcd < 0.001.

3.3. TGL-HDLp interaction

Apolipoprotein I and II (apoLp I/II) – the structural apolipoproteins of lipophorin (HDLp) – were identified as TGL interacting proteins (Table 1, Figs. 6B and 7). ApoLp I/II are synthesized in the fat body from a common precursor which transforms into apoLp-I and -II after post-translational cleavage. InManduca, apoLp I/II were also found associated to LD, the cytosolic organelles housing cellular TG stores[54]. Since apoLp I/II interact with both TGL and LD suggests that HDLp could play a role in the intracellular traffic of DG. The mechanism by which DGs are transported inside the cell from the lipid droplets to the plasma membrane remains unknown. First we examined the intracellular localization of HDLp, DG and TG. Fat body homogenate was subjected to ultracentrifugation in a discontinuous sucrose gradient and the distribution of HDLp (apoLps) along the density gradient was obtained by Western blot (Fig. 12A). The distribution of DG (Fig. 12B), TG (Fig. 12C) and total protein among the fractions was also determined. As expected, a small but significant amount of lipophorin was found in the lipid droplet fraction (fraction 1, 0% sucrose), which contains most of the TG and DG of the fat body. Another small

fraction of lipophorin was found floating at ~20% and ~40% sucrose where plasma membrane and other membranes are expected (fractions 4 and 6). Most of the lipophorin was detected at the bottom of the gradient in the cytosolic fraction (fraction 7) where most of the cellular proteins were also present (not shown). The distribution of intracellular DG was similar to the distribution of lipophorin (Fig. 12B and C).

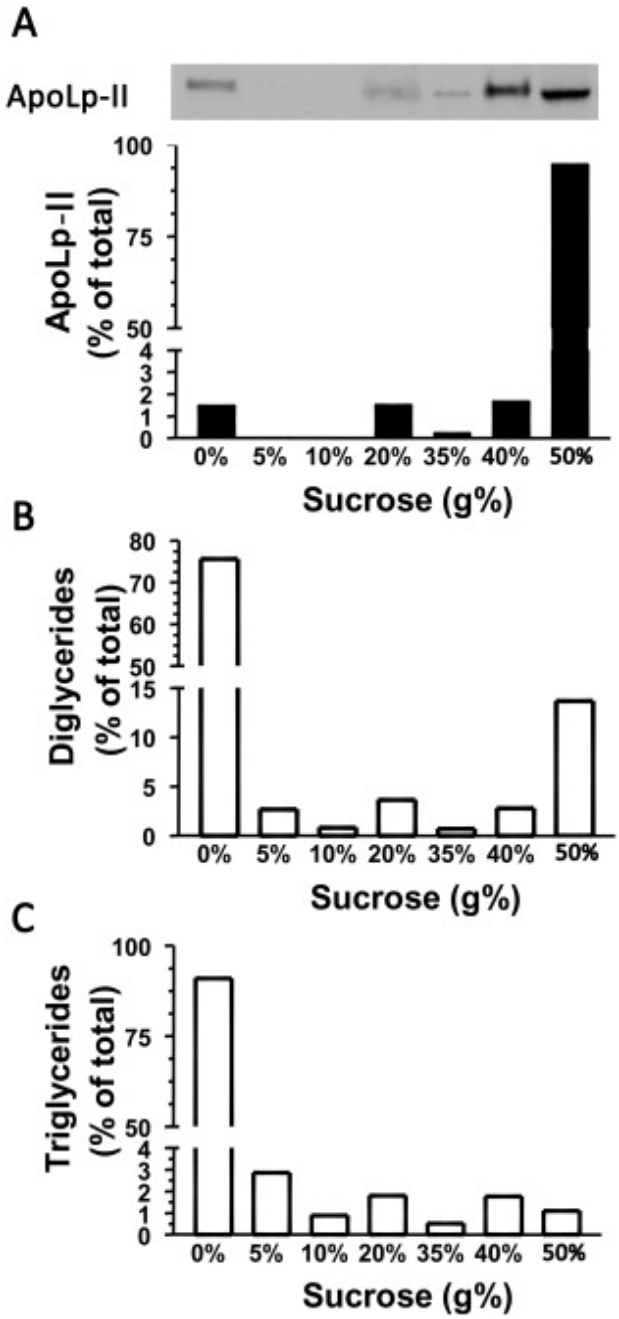

Fig 12. Subcellular distribution of lipophorin, DG and TG. Fat body homogenate from adult male insects was subjected to ultracentrifugation in a sucrose gradient. The gradient was fractionated into seven fractions. The distribution of ApoLp-I/II, DG and TG is shown in panel A, B and C, respectively. Top panel shows a representative western blot depicting the distribution of ApoLp-II among fractions. For this purpose, 0.6% of fraction 1 to 6, and 0.1% of fraction 7 were loaded in 4–20% acrylamide gel, transferred to nitrocellulose and analyzed by western blotting. The concentration of sucrose of the fractions is given in g/100 ml. Panel A graph comes from the densitometry of the blot; panel B and C were obtained after separation of lipids by TLC as described under Materials and Methods. After visualizing lipids spots with iodine, plates were scanned and lipids quantified with AlphaEaseFCTM software. TG and DG contents were expressed as percentage of total neutral lipid. Two independent experiments were carried and Fig. 12 shows a representative result.

Previous studies showed that TGL is always detected in the cytosol. The lipase hydrolyzes TG contained in the lipid droplets but the interaction between TGL and LD is transient[9]. Results shown in Fig. 12 confirmed that HDLp is found in the cytosol. On the other hand, the studies in which we observed the interaction of TGL and HDLp were conducted with the soluble fraction of the fat body indicating that the cytosolic fraction of HDLp interacts with TGL (Figs. 6 and 7).

Because lipophorin is synthesized in the fat body[71], finding intracellular lipoprotein in fat body adipocytes is somehow expected. The pathway of Lp synthesis and secretion in insects has been proposed to be similar to that in mammals[72]. Thus, newly formed lipoprotein is expected to undergo vesicular transport from the ER through Golgi followed by the release of the secretory

vesicles to the hemolymph. However, a very significant amount of Lp was found in the cytosol. The origin of cytosolic Lp is unclear and may be different from the origin of the nascent particle that is secreted to the hemolymph as a particle with low lipid content. Perhaps cytosolic HDLp could come from the hemolymph for reloading of the lipid cargo. It could be transporting intracellular DG from the lipid droplet – the site in which TGL acts – to the plasma membrane for secretion into circulation.

Circulating Lp unloads lipids into the different tissues and the remaining particle returns to the fat body where it is re-loaded with lipids and starts a new cycle of DG transport[72]. Because the turnover of DG occurs at a much higher rate than that of the protein component of lipophorin, a characteristic feature of Lp is that it acts as a reusable lipid shuttle[73]. However, the precise mechanism by which lipophorin reloads the lipid cargo is not completely understood. The original idea is that DG is transferred at the surface of the adipocytes without internalization of the particle in a process facilitated by lipid transfer particle (LTP)[74]. However, receptor mediated endocytic uptake of HDLp also occurs in the fat body of insects[75]. This process is mediated by the lipophorin receptor (LpR). So far the intracellular route of endocytosed Lp is unknown but it appears that the particle is recycled avoiding degradation in lysosomes. The Lp taken up by adipocytes perhaps re-loads lipids at the surface of the lipid droplet in a process mediated by lipases such as TGL. Consistent with this notion, the fat body DG pools that are secreted to the hemolymph seem to localize mainly in the lipid droplets and cytosol.

3.3.1. Effect of HDLp on lipase activity

To gain insight into the possible role of cytosolic Lp on lipid mobilization we investigated whether Lp affects the catalytic properties of TGL. We previously showed that TGL is able to hydrolyze TG to 2-monoacylglycerol (MG), and we asked if the interaction between TGL and

HDLp would impact the hydrolysis products of TG. The activity of partially purified TGL was assayed against [3H]-triolein (25 nmoles) in the presence of increasing amounts of lipophorin (0, 1, 3 and 5 μg of HDLp) that was isolated and quantified as described under Materials and Methods. Following the lipase reaction, lipids from the reaction mixture were extracted by organic solvent and analyzed by TLC to quantify the products of hydrolysis. The amount in nmoles of DG and MG produced during the reaction as well as the amount of TG consumed is shown Fig. 13A. The addition of HDLp altered the properties of TGL as judged by the ratio of [3H]-MG to [3H]-DG produced. In the absence of HDLp this molar ratio was about ~20 but gradually decreased to 2 when the lipase assay was carried out in the presence of 5 μg of HDLp. Control experiments were carried out using bovine albumin (BSA). Addition of increasing amounts of BSA into the assay mixture did not change the lipase activity or the product of hydrolysis (not shown). However, the addition of lipophorin to the assay mixture had an inhibitory effect on the lipase activity. Lipophorin inhibits mostly the DG-lipase activity of TGL, as seen by the decrease in MG production as the concentration of lipophorin is increased. This effect changes the proportion of products formed favoring the production of DG. Previous studies have suggested that most of the DG is found in the core of HDLp particles[76].It seems possible that once DG is formed is somehow shielded in the particle preventing further lipase action.

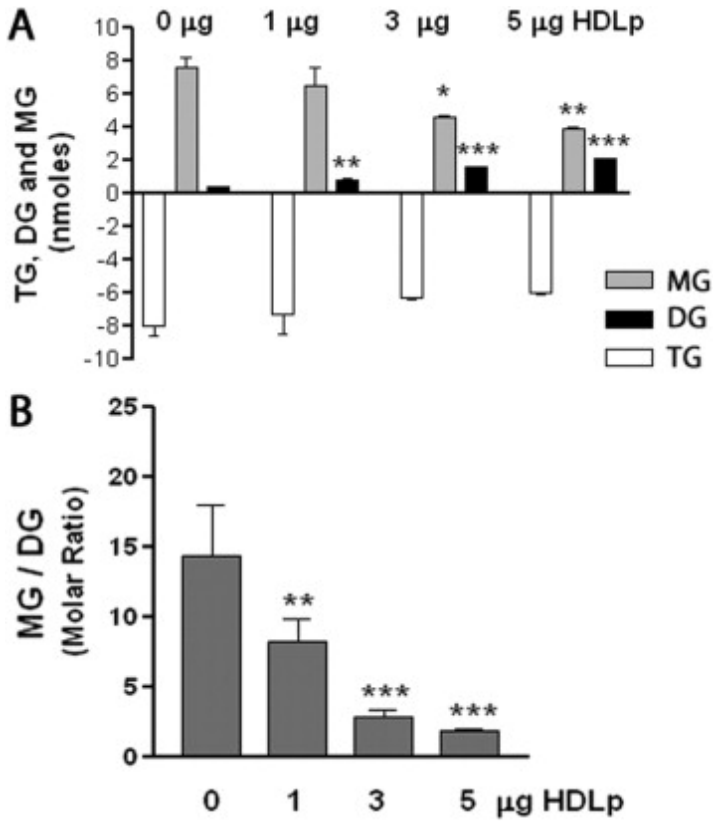

Fig 13. Effect of lipophorin on the lipase activity of TGL. A) The lipase activity of partially purified lipase was determined by incubating 25 nmoles of [3H]-triolein-Triton X-100 with 15 µg of TGL in the presence of increasing amounts of lipophorin (HDLp; δ = 1.15 g/cm3) for 30 min. The formation of individual products (DG, MG) was determined after analyzing the reaction products by TLC coupled to scintillation counting. A) Data representative of one experiment are shown in panel A. Data were expressed in nmoles and are represented as the mean ± SEM of three determinations; B) The effect of lipophorin concentration on the molar ratio DG to MG produced were calculated from the data shown in panel A.

When the organism needs to utilize fatty acids stored in the fat body as TG, the fat body secretes DG into the hemolymph where they are transported by lipophorin to the utilization sites, e.g.

flight muscle. The loading of lipids in the fat body cell is not completely understood. The interaction of TGL with HDLp is significant for two reasons: 1) HDLp modifies the catalytic properties of TGL leading to a higher production of DG; 2) the interaction may be involved in the process of lipoprotein assembly and loading with DG. HDLp could participate in the transport of DG from the lipid droplet – the site in which TGL acts – to the plasma membrane to be secreted into the hemolymph. Finding HDLp in the cytosol, and most importantly, knowing that HDLp interacts with TGL, suggests that lipophorin could take a role in the intracellular transport and/or loading of DG. Future work will be aimed to define the mechanism of intracellular transport and secretion of DG.

CHAPTER III

Study of Mono- and Diacylglycerol Acyltransferases in *Manduca sexta*

1.Introduction

Triacylglycerol [5] is a non-polar acyl triester of glycerol and fatty acids[77]. As a major class of neutral lipid, the presence of TG is widespread in eukaryotes including animals, plants and insects. Insects, as most animals, store large amounts of energy in the form of TG. The main tissue for TG storage in insects is the insect fat body[6]. TG molecules are stored in cytosolic organelles called lipid droplets that besides serving as reservoirs of fatty acids (FA) play a role in the regulation of the metabolism of TG[41]. Utilization of the stored FA requires hydrolysis of the TG molecules by lipases. The lipolytic action releases FA that can thus be further processed by fat body adipocytes to produce acetyl-CoA or other lipids, such as hydrocarbons, waxes, phospholipids or, the most common product, DG. It is in the production of large quantities of DG, and the large concentration of sn-1,2-DG in hemolymph[37], that most insects show a clear difference with the metabolism of lipids in vertebrates. Fat body adipocytes not only produce massive amounts of DG, but they also have the ability to export DG to circulating lipoproteins.

The main insect lipoprotein, lipophorin, is the carrier of the secreted DG and transports the FA to the sites of utilization, such as muscles and ovary[4]. Contrarily to human apoB containing

lipoproteins, lipophorin particles pick up and deliver DG molecules without compromising the integrity of the apolipoproteins. Since the apolipoproteins are recycled, this process is known as the lipophorin shuttle system[73].The ability to secrete DG is not restricted to the fat body. The insect midgut also produces large amounts of DG that are secreted and transported by lipophorin to the fat body. Monoacyglycerol acyltransferases (MGATs) and diacylglycerol acyltransferases (DGATs) catalyze two consecutive steps of enzyme reactions in the synthesis of triacylglycerols (TAGs)[38]

The secretion and transport of DG are salient features of insects and represent a major difference with the mechanisms of FA mobilization and transport in vertebrates. The adipose tissue of vertebrates releases free fatty acids, FFA, which bind to albumin and are transported to other tissues through blood. Liver and intestine of vertebrates release TG into circulation, but this process requires the concomitant synthesis of apolipoprotein B and the intracellular assembly of lipoproteins. On the other hand, the insect midgut secretes DG, but does it without synthesizing a lipoprotein. The unique large production of DG that the fat body and midgut tissues of insects achieve is highly interesting. However, very little is known about the metabolic pathways and genes involved in the synthesis of glycerides.

A major pathway in the synthesis of glycerides in animals is the monoacylglycerol pathway. In this pathway DG synthesis from MG and acyl-CoA is catalyzed by monoacylglycerol acyl transferase, MGAT (EC 2.3.1.22). Subsequent acylation of the DG in a reaction catalyzed by diacylglycerol transferase, DGAT (EC 2.3.1.20), produces TG. In vitro studies have shown that 2-MG is the main product of TG hydrolysis in fat body[8] and therefore suggested that the MG-pathway could be a major route in the synthesis of DG for export. MGAT activity has been

experimentally observed in fat body of several insects[11]. In vitro studies have shown that MGAT activity from M. sexta fat body produces sn-1,2-DG. The production of DG is dependent on the activities of both MGAT, produces DG, and DGAT, consumes DG. In spite of the importance of these genes to the production of DG and the mobilization of FA in insects very little research focusing on acyltransferases has been reported.

In order to further expand our understanding of the synthesis of sn-1,2-DG by the fat body, we took advantage of the information provided by the *Manduca* genome to identify and clone two transcripts that are homologues of the well characterized vertebrates' MGATs and one transcript of M. sexta DGAT that is homologue of the vertebrates DGAT1. In this way, we characterized and compared the acyltransferases gene products from *Manduca sexta* and the predicted acyltransferases from a number of insects whose genomes have been sequenced.

2.Experiment Procedures

Data sources and sequence retrieving

DGAT and MGAT gene and protein sequences were obtained by performing blast searches (blastp, blastx and tblastx) of the Protein and Genome databases at the NCBI (National Center for Biotechnology Information) and the Flybase.

Sequence Alignments

Nucleotide and protein sequences were aligned using the Alignment Explorer/CLUSTALW[78]. The multiple alignments were manually inspected and edited, and only positions unambiguously aligned were included in the final analysis. The default presets for gap penalties and iterations were used for aligning the sequences.

Gene structural analyses

The structural organization of the DGAT and MGAT genes was determined after alignment of genomic DNA and cDNA and EST sequences.

Properties of Predicted Proteins.

The number and location of transmembrane helices (TMH) was predicted using the tools from the Center for Biological Sequence Analysis, Technical University of Denmark (www.cbs.dtu.dk/services/TMHMM) .

Phosphorylation sites were located using the publicly available search programs: Scansite at http://scansite.mit.edu and NetPhos at http://www.cbs.dtu.dk/services/NetPhos/.

3.Results and Discussion

Msex DGAT-1 gene

The candidate gene for DGAT-1 (Msex009756, scaffold000220) was predicted on the basis of its similarity to the best characterized human and mouse DGAT1 protein sequences. A blast search of the Manduca genome database, using as queries the human proteins NP_036211.2 and the mouse proteins NP_034176.1, rendered two Msex cufflinks (Cuffl 19393) coding for putative DGAT1 proteins of 483 and 492 residues. Since the predicted DGAT1 transcripts share identical 3'- and 5'UTRs, in order to clone these transcripts we designed primers targeting the common UTRs. We were able to obtain a single full-length clone of 1583bp encoding a protein of 483 amino acid residues (Figure 14). The predicted MsexDGAT1 protein sequence is 44% identical

(73% similarity) to the sequences of the characterized human and mouse DGAT1 proteins (NP_036211.2; EDL29575.1), Figure 15. Because mouse and human DGAT1 are nearly identical, in Fig.15 we only used the sequence of the human protein for comparison with MsexDGAT. The length of MsexDGAT (483aa) is similar to that of vertebrates' DGAT1 (488aa for human). Two conserved regions that have been mentioned as potential acyl-CoA and DG binding sites are also present in MsexDGAT. These two conserved motifs are characterized by the sequences FYXDWWN, for acyl-CoA binding [14], and HXXXXRHXXXP, for DG binding [15]. Moreover, as shown in the Figure 15 MsexDGAT contains the same number, 9, and location of predicted transmembrane helices (TMH) as the vertebrates' DGAT1. The C-terminal region of MsexDGAT1 (255-483) contains five TMH that constitute the conserved MBOAT domain (pfam03062) found in a number of acyltransferases [16]. The PI (9.34) and mass (57,152 Da) of MsexDGAT are in agreement with the values of vertebrates DGAT1 and also of other predicted insect DGAT1 (Table 3).

```
gctggccgcaaaattttatgaagtaagcggaaagtattatttcaagaaaatgactacggaa
  L  A  A  K  F  Y  E  V  S  G  K  Y  Y  F  K  K  M  T  T  E
gatgaagacaaagcgctacgatacagaagagcccaaagtgttactcgggctgaagaaata
 D  E  D  K  A  L  R  Y  R  R  A  Q  S  V  T  R  A  E  E  I
tctgaacaagaaaaaaaagtacgaaggtcacagcttgataaaccaattcacaaaccacgg
 S  E  Q  E  K  K  V  R  R  S  Q  L  D  K  P  I  H  K  P  R
gattcacttttctcatggagttcagagtttacaaactttactggtttggttaattggggt
 D  S  L  F  S  W  S  S  E  F  T  N  F  T  G  L  V  N  W  G
ttcttgatgcttactattggcggtgtgaggctaggacttgaaaacttttaaaatacggt
 F  L  M  L  T  I  G  G  V  R  L  G  L  E  N  F  L  K  Y  G
tttcgtgtgaatcccatcgagtggatcatagttttaactggataccatgaaggagataaa
 F  R  V  N  P  I  E  W  I  I  V  L  T  G  Y  H  E  G  D  K
tatcagtatccgtcgcttgcgctgataatgtttgctgttgtaccgccagttatagcacta
 Y  Q  Y  P  S  L  A  L  I  M  F  A  V  V  P  P  V  I  A  L
cttatagaaaaagcaattgcagtggatttgattccacagaagattggcatgtccatacaa
 L  I  E  K  A  I  A  V  D  L  I  P  Q  K  I  G  M  S  I  Q
atcgcgaacatattgtttgttgtttccctgcctgctattgtgcttcattttaaaggagac
 I  A  N  I  L  F  V  V  S  L  P  A  I  V  L  H  F  K  G  D
gattttagttttgtcggtataactacagtatgtatgttatatttagtaattttcctcaaa
 D  F  S  F  V  G  I  T  T  V  C  M  L  Y  L  V  I  F  L  K
ttatggagttacacgcaaaccaactattggtgcagatgtggtacgaagcgcaagttgtct
 L  W  S  Y  T  Q  T  N  Y  W  C  R  C  G  T  K  R  K  L  S
aagaacacattgaggagacaaagcctgtcagcacctacatggaaaagttttgaagacgag
 K  N  T  L  R  R  Q  S  L  S  A  P  T  W  K  S  F  E  D  E
aagaatgaagcagctgtcgcggttggacttgtcaaatatccagataacttgaatttgaag
 K  N  E  A  A  V  A  V  G  L  V  K  Y  P  D  N  L  N  L  K
gatctgttctatttcttgttggcccctactctatgttacgaattgaacttcccacgcacg
 D  L  F  Y  F  L  L  A  P  T  L  C  Y  E  L  N  F  P  R  T
gcacgtattaggaagaggttcctcgtcaaaagattacttgaagtggtgtttggattaaac
 A  R  I  R  K  R  F  L  V  K  R  L  L  E  V  V  F  G  L  N
ctggtcttagcattgttccagcaatggatgataccctcagtgaccaattcgatcgacacg
 L  V  L  A  L  F  Q  Q  W  M  I  P  S  V  T  N  S  I  D  T
ttctctacaatggatcctatcagaataacggagcgacttttgaaattggccgtaccgaac
 F  S  T  M  D  P  I  R  I  T  E  R  L  L  K  L  A  V  P  N
catcttatatggctatgcttcttctacctaagcttccactcgtttttaaacctcatgggt
 H  L  I  W  L  C  F  F  Y  L  S  F  H  S  F  L  N  L  M  G
gagttgctccaatttgccgatcgtaatttctataacgattggtggaacgcgaacaatata
 E  L  L  Q  F  A  D  R  N  F  Y  N  D  W  W  N  A  N  N  I
tcagtgttttggagtacttggaacatgcccgtgcacatgtgggcggtgagacacgtctac
 S  V  F  W  S  T  W  N  M  P  V  H  M  W  A  V  R  H  V  Y
ataccgatcactaagcgaggtcacagcaaagtggttgctagtattgtcgttttcttcata
 I  P  I  T  K  R  G  H  S  K  V  V  A  S  I  V  V  F  F  I
tcggcgttcttccacgagtatttggtgagcgtaccattgcagatgtttaggatctgggca
 S  A  F  F  H  E  Y  L  V  S  V  P  L  Q  M  F  R  I  W  A
ttcttgggcatgatggcccagcctcccctatcggttatttctcgcatggccgagataaag
 F  L  G  M  M  A  Q  P  P  L  S  V  I  S  R  M  A  E  I  K
ctgggcccacgttggggcaacctgatagtgtggagttcactgatcttgggccagcctctc
 L  G  P  R  W  G  N  L  I  V  W  S  S  L  I  L  G  Q  P  L
gctatcatgatgtactatcacgactacgctctcttgcacttcactcctgcaaagttataa
 A  I  M  M  Y  Y  H  D  Y  A  L  L  H  F  T  P  A  K  L  -
tatttatatattaactgttgatatttttatattcaataatggtgtttttctttcctctca
 Y  L  Y  I  N  C  -  Y  F  Y  I  Q  -  W  C  F  S  F  L  S
ttattcaacgattccagaaacg
 L  F  N  D  S  R  N
```

Figure 14. DNA and protein sequence of MsexDGAT1. The figure shows the DNA and predicted ORF amino acid sequence of the Msex DGAT1 cloned in this study. Start and stop codons are highlighted.

```
Human DGAT1     MGDRGSSRRRRTGSRPSSHGGGGPAAAEEEVRDAAAGPDVGAAGDAPAPAPNKDGDAGVG 60
Msex  DGAT1     MTTEDEDKALRYRRAQSVTRAEEISEQEKKVR--------------------------- 32
                *  ....:  *     *   .   :  *::**

Human DGAT1     SGHWELRCHRLQDSLFSSDSGFSNYRGILNWCVVMLILSNARLFLENLIKYGILVDPIQV 120
Msex  DGAT1     RSQLDKPIHKPRDSLFSWSSEFTNFTGLVNWGFLMLTIGGVRLGLENFLKYGFRVNPIEW 92
                 .: :   *: :***** .* *:*: *::** .:** :...** ***::***: *:**:

Human DGAT1     VSLFL----KDPYSWPAPCLVIAANVFAVAAFQVEKRLAVGALTEQAGLLLHVANLATIL 176
Msex  DGAT1     IIVLTGYHEGDKYQYPSLALIMFAVVPPVIALLIEKAIAVDLIPQKIGMSIQIANILFVV 152
                : ::      * *.:*: .*:: * * .* *: :** :**. :.:: *: :::**:  ::

Human DGAT1     CFPAAVVLLVES-ITPVGSLLALMAHTILFLKLFSYRDVNSWCRR----------ARAKA 225
Msex  DGAT1     SLPAIVLHFKGDDFSFVGITTVCMLYLVIFLKLWSYTQTNYWCRCGTKRKLSKNTLRRQS 212
                .:** *: :  . :: **   . * : ::****:** :.* ***           * ::

Human DGAT1     ASAG-------KKASSAAAPHTVSYPDNLTYRDLYYFLFAPTLCYELNFPRSPRIRKRFL 278
Msex  DGAT1     LSAPTWKSFEDEKNEAAVAVGLVKYPDNLNLKDLFYFLLAPTLCYELNFPRTARIRKRFL 272
                 **        :* .:*.*   *.*****. :**:***:***********:.*******

Human DGAT1     LRRILEMLFFTQLQVGLIQQWMVPTIQNSMKPFKDMDYSRIIERLLKLAVPNHLIWLIFF 338
Msex  DGAT1     VKRLLEVVFGLNLVLALFQQWMIPSVTNSIDTFSTMDPIRITERLLKLAVPNHLIWLCFF 332
                ::*:**::*  :* :.*:****:*:: **:..*. **  ** *************** **

Human DGAT1     YWLFHSCLNAVAELMQFGDREFYRDWWNSESVTYFWQNWNIPVHKWCIRHFYKPMLRRGS 398
Msex  DGAT1     YLSFHSFLNLMGELLQFADRNFYNDWWNANNISVFWSTWNMPVHMWAVRHVYIPITKRGH 392
                *  *** ** :.**:**.**:**.****::.:: **..**:*** *.:**.* *: :**

Human DGAT1     SKWMARTGVFLASAFFHEYLVSVPLRMFRLWAFTGMMAQIPLAWF--VGRFFQG-NYGNA 455
Msex  DGAT1     SKVVASIVVFFISAFFHEYLVSVPLQMFRIWAFLGMMAQPPLSVISRMAEIKLGPRWGNL 452
                ** :*   **: *************:***:*** ***** **: :  :..:  * .:**

Human DGAT1     AVWLSLIIGQPIAVLMYVHDYYVLNYEAPAAEA 488
Msex  DGAT1     IVWSSLILGQPLAIMMYYHDYALLHFTPAKL-- 483
                 ** ***:***:*::** *** :*:: ..
```

Figure 15. Sequence alignment of Human DGAT1 (NP_036211.2) and MsexDGAT1 (KF800701). Underlined are two regions that have been proposed as potential acyl-CoA and DG binding sites. These two conserved motifs are characterized by the sequences FYXDWWN, for acyl-CoA binding (Yen et al. 2008) and HXXXXRHXXXP, for DG binding (Xu J et al 2008).

	Hs	Mm	Dp	Hm	Msex	Bm	Tc	Dm	Bt	Ag	Aae
Human	10	86	44	46	46	47	45	44	45	46	47
Mouse	86	100	43	45	46	46	45	44	45	46	46
Dp	44	43	100	82	80	77	61	63	62	64	67
Hm	46	45	82	100	78	79	61	60	61	63	63
Msex	46	46	80	78	100	82	60	62	61	63	64
Bm	47	46	77	79	82	100	58	60	57	61	63
Tc	45	45	61	61	60	58	100	63	68	65	69
Dm	44	44	63	60	62	60	63	100	65	68	70
Bt	45	45	62	61	61	57	68	65	100	70	71
Ag	46	46	64	63	63	61	65	68	70	100	85
Aae	47	46	67	63	64	63	69	70	71	85	100
Mass	55.	56.8	55.2	57.1	57.1	56.7	56	54.7	56.7	54.9	55.3
Isoelect.	9.4	9.41	9.53	9.19	9.34	9.46	9.29	9.26	9.47	9.39	9.71

Table 2.

Identity Matrix, Masses and Isoelectric points of DGAT1. Highlighted in yellow are the cross identities among Lepidoptera DGAT1 proteins. Human: Homo sapiens DGAT1, NP_036211.2; Mouse: Mus musculus,EDL29575.1; Msex: Manduca sexta DGAT1 gb: KF800701; Bm: Bombyx mori; gi512909843, XP_004927020.1, Pred. DGAT1-like isoform X1; Dp: Danaus plexipus; gi357623602, gb:EHJ74688.1, Pred.sterol o-acyltransferase; Hm: Heliconius melpomene gnl|BL_ORD_ID|7464 HMEL011652;Dm: Drosophila melanogaster;gi19921444, NP_609813.1 midway, isoform A; Ag: Anopheles gambiae; gi 158297422, XP_317656.3, AGAP007843-PA; Aea: Aedes aegypti gi157115823, XP_001658299.1, sterol o-acyltransferase; Tc: Tribolium castaneum; gi 91083363, XP_975142.1, Pred: sterol o-acyltransferase; Bt: Bombus terrestris gi340723317;XP_003400037.1 Pred: DGAT1-like

A comparison of MsexDGAT1 with the predicted homologues from eight different insects (Figure 16) shows that the protein is highly conserved (42.4% overall identity and 69%

similarity). The conservation extends to the location and number of TMHs (not shown). As expected, if the comparison is limited to species of Lepidoptera (Bombyx mori, Danus plexipus, Heliconius melpomene and Manduca sexta) the similarity of the sequences increases to 89% (Figure 17) and the identity to 78-82% (Table 2).

```
Tc              -----EQE---GIRYRRAQSVTRAEEIQAVKQKVRKSQPDKPIHKPRDSLLSWNSGFENF 52
Bt              --MTIEHENDTKVRLRRTKSVTRAEEIQKAEMLARKSQPDKPCHRPRDSLFSWSSGFGNF 58
Ag              -EEN-------KVRYRRTQSVTRAEEITKKESEQRKSQPDKPCHRPRDSLFSWSSGFDNF 52
Aea             --DN-------KVRYRRTQSVTRAEEITKKESKERKSQPDKPCHRPRDSLFSWSSGFDNF 51
Dm              --TNGSEK---KLRYRRTQSVTRAEEISNKEEKQRRAQPGRPIHRPRDSLFSWSSGFTNF 55
Msex483         MTTEDEDK---ALRYRRAQSVTRAEEISEQEKKVRRSQLDKPIHKPRDSLFSWSSEFTNF 57
Bm              MMTETEDK---TLRYRRAQSVTRAEEITEKEKKVRSSQLDKPIHKPRDSLFSWSSEFANF 57
Dp              --SNKEEN---ALRYRRAQSVTKAEEITEKEKKARNSQLDKPIHKPRDSLFSWSSEFTNF 55
Heliconius      MPSKIEES---SLRYRRAQSVTKAEEITEKEKKARNSQLDKPCHKPRDSLFSWSSEFTNF 57
                          :* **::***:****   :   * :* .:* *:*****:**.* * **

Tc              TGFVNWAFLLLSIGGLRLLLENFIKYGIRVDPVQWFYILTGQDEQ-GTEHPSIVLILYSV
111
Bt              TGFVNWGFLLLGIGGIRLLLENFIKYGLRVDPWEWFLFFSGKYEG-GEEHPSILLIIYST
117
Ag              TGLVNWGFLLLTMGGIRLVLENFIKYGIRVDPVQWFTVLTGKGE--GEGYPSVLLISYSL
110
Aea             TGLVNWGFLLLTMGGFRLVLENFIKYGIRVDPVQWFVVLTGRNE--GQGHPSLLLILYSI
109
Dm              SGLVNWGFLLLCIGGLRLGLENLLKYGIRINPLDWFFFISGHNE--GEGHNALILSIYSL
113
Msex483         TGLVNWGFLMLTIGGVRLGLENFLKYGFRVNPIEWIIVLTGYHEGDKYQYPSLALIMFAV
117
Bm              TGLVNWGFLMLTVGGVRLCLENFLKYGFRVNPIEWIIVLTGYNEGHSHQYPSVVLLIFSI
117
Dp              TGLVNWGFLLLTIGGVRLCLENFLKYGIRVNPFEWIIVVTGYHEGQSHQYPSVILLIFSV
115
Heliconius      TGLVNWGFLMLTIGGLRLCLENFLKYGIRVNPFEWIIVLTGYNEGYSHQYPSVILLIFSV
117
                :*:***.**:* :**.** ***::***:*::* :*: ..:*  *     : :: *  ::

Tc              VPIIFCLLTEKALAVEIISRRMGMMMHVVNLLVLIFLPMVVIHYKD-GFSLVGASTVTTL
170
Bt              VPIGLCLLIEKGLSVDIIAHEPGMVFHVVNLIVMVLVPMVVIHVKDSGFSLFGAMYVCML
177
Ag              VPVMICLMMERALASDIIPESAGMAVHIVNIIVLVLIPMVVIHVKGHIFSLVGAMTVCFI
170
Aea             VPILICLMVEKGLASEVIMESAGMIVHVVNILVLVLIPMVVIHVKGQAFSLVGAMTVCFV
169
Dm              VHISLCLAVEKGLAMEIIAEGLGLFIQIVNIVVLVCLPVVTIHLKGHAFSLMGASTVCFF
173
Msex483         VPPVIALLIEKAIAVDLIPQKIGMSIQIANILFVVSLPAIVLHFKGDDFSFVGITTVCML
177
Bm              VPTVVALMIEKGIAVNLINEKLGVFLQITNILFIITLPAVVLQIKGNHFSFIGATTVCMI
177
Dp              VPAVFALLVEKAIARDVISSKMGVSVQIFNIISTVSLPVIVLNFKGQQFSFVGITTVCLI
175
Heliconius      VPAVVSLLIEKAIAVEILSQKIGVTLQIINLLSEITLPVVVLYFKGDEFSFVGSSTVCMI
177
                *   ..*  *:.:: :::    *: .:: *::  : :* :.:  *.  **:.*   *  .

Tc              YSVLFLKLWSYVQVNLWCRN-ARQSSNNKS-LRRQSLSYNNLPKDEDSNKNHKDSKDDLS
228
```

```
Bt              YAILFLKLWSYVQVNMWCRLGARRKAKSQGRMRRKSLSCDNLQSSIAKKNGDLVHNSKHK
237
Ag              YCILFLKLWSYVQVNLWCRA-EKKQHRHSRSGRRQSITIAQLR--NATGYCN--DKDKVP
225
Aea             YCILFLKMWSYVQVNLWCRN-QYKHSRK-RSGRRQSISIAQLRRQNGNGVATGAEKDKVP
227
Dm              YSVLFLKLWSYVQTNMWCRQ---TYYQKNPRERRPSITLAELKKGVLNGGEE---DEDVS
227
Msex483         YLVIFLKLWSYTQTNYWCRC-GTKRKLSKNTLRRQSLSAPTW---------KSFEDEKNE
227
Bm              YLILFLKIWSYSQTNYWCRN-GTKNRFSKNKLRRQSLSAPNWSKLVNAEQDQTYEEEKNE
236
Dp              YLVLFLKLWSYVQTNHWCRQ-GMKAKQFKNKLRRQSLSAPNWKS----------EDDID-
223
Heliconius      YLVLFLKLWSYCQTNHWCRR-VMRSKQYKNSLRRQSLSAPNWNELVNADQDQSHEDEKND
236
                * ::***:*** *.* ***             ** *::                ..

Tc              N-TERLLVQYPDNLNLRDLFYFLCAPTLCYELNFPRTERIRKRFLLKRIFEVLAGIQLIL
287
Bt              V-DGMVLVQYPDNLNLRDLYYYILAPTLCYELNFPRTQRIRKRFLIKRILEVVVGLQVVM
296
Ag              -----ALVHYPDNLHPVDLFYFLLAPTLCYELNFPKTNRIRKRFLIKRMLEVVIGVHIVM
280
Aea             -----KLVHYPDNLHLKDLFYFLLAPTLCYELNFPRTSRIRKRFLIKRILEVVIGVHIVM
282
Dm              -----KLVQYPDNLTYKDLLYFLCAPTLCYELNFPRTSRVRKRFLLKRLLEVVIGVNVVM
282
Msex483         AAVAVGLVKYPDNLNLKDLFYFLLAPTLCYELNFPRTARIRKRFLVKRLLEVVFGLNLVL
287
Bm              EAAAAGLIKYPNNLTLKDLFYFLLAPTLCYELNFPRTARIRKRFVVKRLVELAFGVNLVL
296
Dp              --LSPGLVKYPHNLNLKDLFYFLLAPTLCYELNFPRTTRIRKRFLIKRLLEVVFGINLVL
281
Heliconius      -VASSGLVKYPDNLNLKDLFYFLLAPTLCYELNFPRTTRIRKRFLIKRIVEVVFGMNLVL
295
                      *::**.**   ** *:: ***********:* *:****::**:.*:  *:::::

Tc              CIFQQYMIPSVKNSLIPFSNMDVALASERLLKLAIPNHLAWLCMFYILFNSWLNLLGEIL
347
Bt              SLFQQWMIPCVKNSLVPFSNMDVAKASERLLKLAIPNHLVWLCFFYLMFHSLLNLMGELL
356
Ag              GLFQQWMIPSVRNSLVPFSNMDLTKTAERLLKLAIPNHLMWLCFFYLTFHSFLNLMGELL
340
Aea             GLFQQWMIPSVKNSLVPFSNMDLTKMTERLLKLAIPNHLMWLCFFYLTFHSFLNLMGELL
342
Dm              ALFQQWIIPSVRNSLIPFSNMDVALATERLLKLALPNHLCWLCFFYLMFHSFLNAVGELL
342
Msex483         ALFQQWMIPSVTNSIDTFSTMDPIRITERLLKLAVPNHLIWLCFFYLSFHSFLNLMGELL
347
Bm              ALFQQWMIPSVTNSVDTFSTMDPIRITERLLKLAVPNHLIWLCLFYLSFHSFLNLMGELL
356
Dp              ALFQQWMIPSVKNAVDPFSELDMIKMTERLLKLAVPNHLIWLCLFYLSFHSFLNLMGELL
341
```

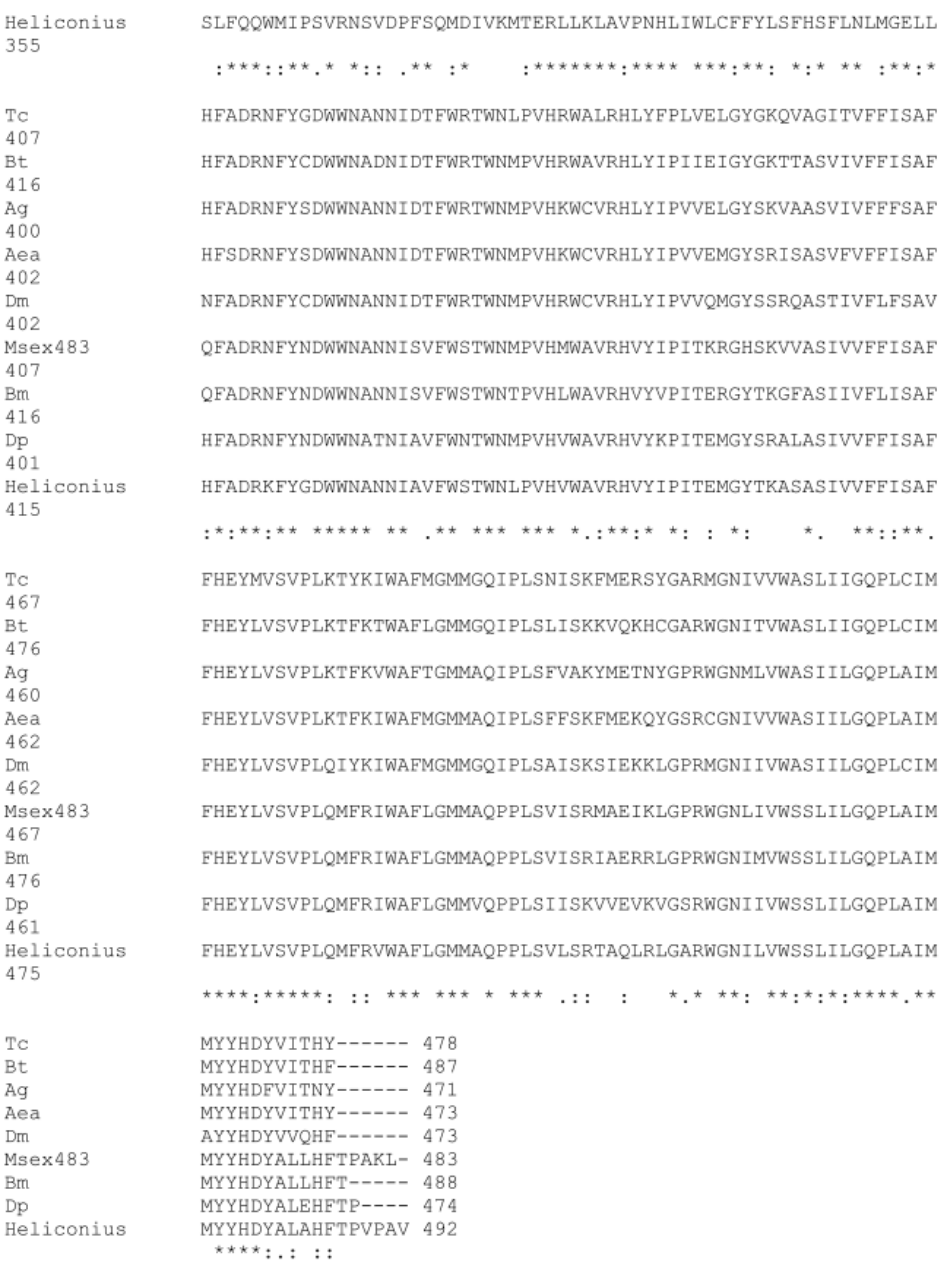

Fig 16. Multiple sequence alignment of insect proteins similar to Manduca DGAT1. The sequences identifiers and abbreviations used are: Msex483: Manduca sexta DGAT1 gb: KF800701; Bm: Bombyx mori; gi512909843, XP_004927020.1, Pred. DGAT1-like isoform X1; Dp: Danaus plexipus; gi357623602, gb:EHJ74688.1, Pred.sterol o-acyltransferase;

Heliconius: Heliconius melpomene gnl|BL_ORD_ID|7464 HMEL011652;Dm: Drosophila melanogaster;gi19921444, NP_609813.1 midway, isoform A; Ag: Anopheles gambiae; gi 158297422, XP_317656.3, AGAP007843-PA; Aea: Aedes aegypti gi157115823, XP_001658299.1, sterol o-acyltransferase; Tc: Tribolium castaneum; gi 91083363, XP_975142.1, Pred: sterol o-acyltransferase; Bt: Bombus terrestris gi340723317;XP_003400037.1 Pred: DGAT1-like.

```
Dp              --SNKEENALRYRRAQSVTKAEEITEKEKKARNSQLDKPIHKPRDSLFSWSSEFTNFTGL
Heliconius      MPSKIEESSLRYRRAQSVTKAEEITEKEKKARNSQLDKPCHKPRDSLFSWSSEFTNFTGL
Msex483         MTTEDEDKALRYRRAQSVTRAEEISEQEKKVRRSQLDKPIHKPRDSLFSWSSEFTNFTGL
Bm              MMTETEDKTLRYRRAQSVTRAEEITEKEKKVRSSQLDKPIHKPRDSLFSWSSEFANFTGL
                  :: *:.:**********:****:*:***.* ****** **************:*****

Dp              VNWGFLLLTIGGVRLCLENFLKYGIRVNPFEWIIVVTGYHEGQSHQYPSVILLIFSVVPA
Heliconius      VNWGFLMLTIGGLRLCLENFLKYGIRVNPFEWIIVLTGYNEGYSHQYPSVILLIFSVVPA
Msex483         VNWGFLMLTIGGVRLGLENFLKYGFRVNPIEWIIVLTGYHEGDKYQYPSLALIMFAVVPP
Bm              VNWGFLMLTVGGVRLCLENFLKYGFRVNPIEWIIVLTGYNEGHSHQYPSVVLLIFSIVPT
                ******:**:**:** ********:****:*****:***.** .:****: *::*::**

Dp              VFALLVEKAIARDVISSKMGVSVQIFNIISTVSLPVIVLNFKGQQFSFVGITTVCLIYLV
Heliconius      VVSLLIEKAIAVEILSQKIGVTLQIINLLSEITLPVVVLYFKGDEFSFVGSSTVCMIYLV
Msex483         VIALLIEKAIAVDLIPQKIGMSIQIANILFVVSLPAIVLHFKGDDFSFVGITTVCMLYLV
Bm              VVALMIEKGIAVNLINEKLGVFLQITNILFIITLPAVVLQIKGNHFSFIGATTVCMIYLI
                *.:*::**.** ::: .*:*: :** *::  ::**.:** :**:.***:* :***::**:

Dp              LFLKLWSYVQTNHWCRQGMKAKQFKNKLRRQSLSAPNWKSEDD------------ID-LS
Heliconius      LFLKLWSYCQTNHWCRRVMRSKQYKNSLRRQSLSAPNWNELVNADQDQSHEDEKNDV-AS
Msex483         IFLKLWSYTQTNYWCRCGTKRKLSKNTLRRQSLSAPTWKS---------FEDEKNEAAVA
Bm              LFLKIWSYSQTNYWCRNGTKNRFSKNKLRRQSLSAPNWSKLVNAEQDQTYEEEKNEEAAA
                :***:*** ***:***   : :  **.*********.*..                  :

Dp              PGLVKYPHNLNLKDLFYFLLAPTLCYELNFPRTTRIRKRFLIKRLLEVVFGINLVLALFQ
Heliconius      SGLVKYPDNLNLKDLFYFLLAPTLCYELNFPRTTRIRKRFLIKRIVEVVFGMNLVLSLFQ
Msex483         VGLVKYPDNLNLKDLFYFLLAPTLCYELNFPRTARIRKRFLVKRLLEVVFGLNLVLALFQ
Bm              AGLIKYPNNLTLKDLFYFLLAPTLCYELNFPRTARIRKRFVVKRLVELAFGVNLVLALFQ
                 **:***.**.********************:******::**::*:.**:****:***

Dp              QWMIPSVKNAVDPFSELDMIKMTERLLKLAVPNHLIWLCLFYLSFHSFLNLMGELLHFAD
Heliconius      QWMIPSVRNSVDPFSQMDIVKMTERLLKLAVPNHLIWLCFFYLSFHSFLNLMGELLHFAD
Msex483         QWMIPSVTNSIDTFSTMDPIRITERLLKLAVPNHLIWLCFFYLSFHSFLNLMGELLQFAD
Bm              QWMIPSVTNSVDTFSTMDPIRITERLLKLAVPNHLIWLCLFYLSFHSFLNLMGELLQFAD
                ******* *::* ** :* :::*****************:***************:***

Dp              RNFYNDWWNATNIAVFWNTWNMPVHVWAVRHVYKPITEMGYSRALASIVVFFISAFFHEY
Heliconius      RKFYGDWWNANNIAVFWSTWNLPVHVWAVRHVYIPITEMGYTKASASIVVFFISAFFHEY
Msex483         RNFYNDWWNANNISVFWSTWNMPVHMWAVRHVYIPITKRGHSKVVASIVVFFISAFFHEY
Bm              RNFYNDWWNANNISVFWSTWNTPVHLWAVRHVYVPITERGYTKGFASIIVFLISAFFHEY
                *:** *****.**:***.*** ***:******* ***: *:::  ***:**:********

Dp              LVSVPLQMFRIWAFLGMMVQPPLSIISKVVEVKVGSRWGNIIVWSSLILGQPLAIMMYYH
Heliconius      LVSVPLQMFRVWAFLGMMAQPPLSVLSRTAQLRLGARWGNILVWSSLILGQPLAIMMYYH
Msex483         LVSVPLQMFRIWAFLGMMAQPPLSVISRMAEIKLGPRWGNLIVWSSLILGQPLAIMMYYH
Bm              LVSVPLQMFRIWAFLGMMAQPPLSVISRIAERRLGPRWGNIMVWSSLILGQPLAIMMYYH
                **********:*******.*****::*: .: ::* ****::******************

Dp              DYALEHFTP----
Heliconius      DYALAHFTPVPAV
Msex483         DYALLHFTPAKL-
Bm              DYALLHFT-----
```

Fig 17. Multiple sequence alignment DGAT1 from Lepidoptera. Msex483: Manduca sexta DGAT1 gb: KF800701; Bm: Bombyx mori; gi512909843, XP_004927020.1, Pred. DGAT1-like isoform X1; Dp: Danaus plexipus; gi357623602, gb:EHJ74688.1, Pred.sterol o-acyltransferase; Heliconius: Heliconius melpomene gnl|BL_ORD_ID|7464 HMEL011652.

Several consensus phosphorylation motifs are present in the N-terminal of MsexDGAT1. Some of these sites are 100% conserved among insect DGAT1 and some are also conserved in mouse and human DGAT1s (Figure 18). The serine residues of MsexDGAT located at positions 17, RRAQSVTRA, 34, KVRRSQLDK, and 46, KPRDSLFSW, highlight highly probable phosphorylation sites clustering in the N-terminal of DGAT1, before the beginning of the transmembrane regions. The PKA phosphorylation motifs centered on serine residues 17 and 46 are also conserved in human and mouse DGAT1. Another pair of conserved and possible PKA phosphorylation sites, S187and S212, is found in the region that separates the two bundles of TMH present in DGAT1.

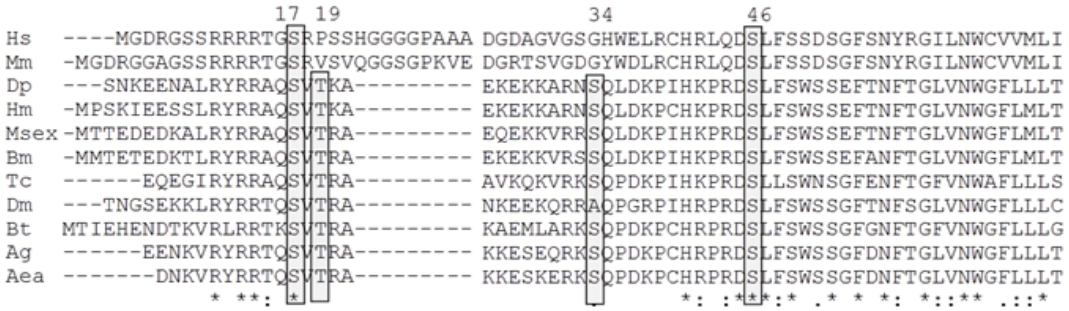

Figure 18. Conserved Phosphorylation Sites Among DGAT1. Alignments were produced

with Clustal Omega. The sequences identifiers and abbreviations used are: Hs: Homo sapiens, NP_036211.2; Mm: Mus musculus,EDL29575.1; Dp: Danus plexipus; gi357623602, gb:EHJ74688.1; Hm: Heliconius melpomene gnl|BL_ORD_ID|7464 HMEL011652; Msex: Manduca sexta; gb: KF800701; Bm: Bombyx mori; gi512909843, XP_004927020.1; Tc: Tribolium castaneum; gi 91083363, XP_975142.1; Dm: Drosophila melanogaster; gi19921444, NP_609813.1; Ag: Anopheles gambiae; gi 158297422, XP_317656.3, AGAP007843-PA; Aea: Aedes aegypti gi157115823, XP_001658299.1; Bt: Bombus terrestris gi340723317;XP_003400037.1. The indicated amino acid position numbers are based on the Msex sequence.

It is also important to note that some of the insect proteins referred to as DGAT1 in the present study have been annotated as sterol o-acyltransferases. This is the case for Danus plexipus, gi357623602, Aedes aegypti, gi157115823, and Tribolium castaneum, gi91083363. However, our study suggested that they are homologues of the DGAT1 from vertebrates.

Two DGAT genes are found in plants, vertebrates and fungi, DGAT1 and DGAT2. These genes encode polypeptides that share a low degree of sequence homology and have a large difference in polypeptide length. MsexDGAT1 is clearly different to human DGAT2 (10% identity). Moreover, DGAT1 is a larger polypeptide (~480-490aa) than DGAT2 (388aa). The structure of DGAT2 is also different. A simple prediction of TMH shows that DGAT2 has only 1 or 2 TMH, whereas DGAT1 is characterized by the presence of 9 TMH. In fact, a search of the Manduca genome rendered no matches that could be confidently considered DGAT2 homologues.

The gene model built in the Manduca Genome Project indicates that the MsexDGAT1 gene has a

length of 9714bps and consists of 12 exons evenly distributed. The MBOAT domain, common to all DGAT1 proteins, is encoded by the last three exons (10-12) of the MsexDGAT gene. A comparison of the gene structures of DGAT1 from several insects and some vertebrates is shown in Fig19. A very similar gene structure is found in other Lepidoptera such as Heliconius melpomene (12 exons of similar size) and Bombyx mori (11 exons, 10 of similar size); the genomic sequence of Danus plexipus DGAT1 (10 exons) may not be complete but the gene organization is still similar to other Lepidoptera's DGAT1. Bombus terrestris DGAT1 gene also has 12 exons. DGAT1 genes of dipterans seem to have a lower number of exons (8 to 10), whereas Tribolium castaneum (only 6 exons) presents clear differences with all other genes. The size of MsexDGAT1 gene is similar to the sizes of human (10,080bps) and murine (9543bps) DGAT1 genes. However, the number of exons in DGAT1 from vertebrates is higher (16-17) and they cluster towards the 3'end. The worm C. elegans DGAT1 gene has only 7 coding exons and a length of 2771bps. Overall the size of the DGAT1 gene show significant variation among insect species.

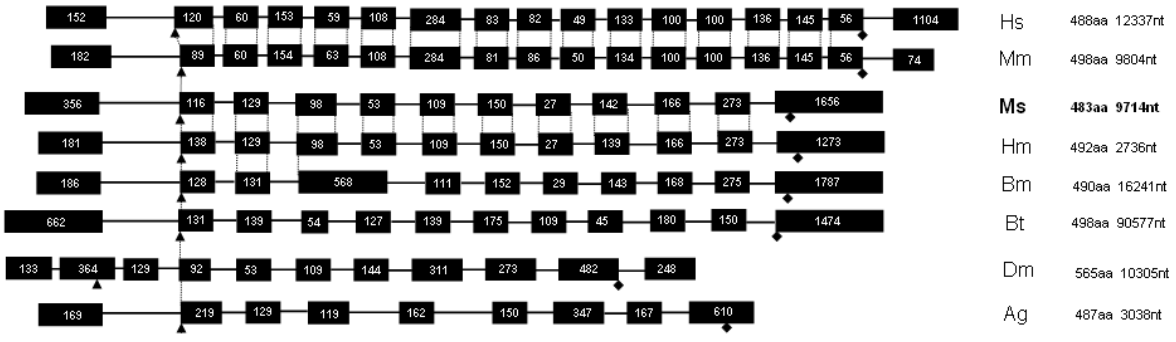

Figure 19. Structure of DGAT1 genes. The figure sketches the structures of DGAT1 genes

from several insect species. Also included are the structures of the DGAT1 genes found in mouse and human genomes. The number and size of the exons and the total gene lengths are indicated. The size of each exon (in bp) is given. Bars represent introns. Start site is marked with arrow head (◂) and stop codon is marked with diamond (◆).

The most common reaction for the synthesis of TG is catalyzed by DGATs using acyl-CoA and DG as substrates. DG can be used for export into the hemolymph or for the synthesis of phospholipids. Thus, the activity of DGAT is important because to a great extent its relative activity defines whether or not the tissue storages FA as TG or, in other words, the fate of DG. Two DGATs, DGAT1 and DGAT2, are found in vertebrates[79]. These two enzymes catalyze the same reaction but have evolved from different ancestral precursors, and have different catalytic properties and physiological functions[80, 81].

Our study suggests that insects lack a homologue of the vertebrates DGAT2. Searches for homologues of human or murine DGAT2 in insects did not provide a convincing match. The predicted insect protein hits from blast searches using DGAT2 as query were actually more similar to MGAT2 than DGAT2 and were missing the N-terminal sequence characteristic of DGAT2. Given the fact that transgenic DGAT2-knockout mice die soon after birth [81]., the apparent lack of DGAT2 in insects is somehow surprising. However, the precise reason why the DGAT2 knockout is lethal to mice is not known. A recent study has shown that adipocytes from DGAT2 knockout mice still accumulate TG to the same extent as wild type adipocytes [82]; therefore, the study suggests that at least in adipose tissue DGAT1 could substitute for the lack of

DGAT2. If both DGAT proteins are knocked out then the adipocytes have no TG indicating that none of the other acyltransferases present in adipocytes can substitute for the DGAT activity. Although further studies are required to confirm the absence of a second DGAT in insects, the current information suggests this would be the case and thus DGAT1 would be the only DGAT gene present in insects.

The comparison of MsexDGAT1 with predicted acyltransferases from a number of insects provided a broad characterization of insect DGAT1. Several of the predicted phosphorylation sites identified were found to be conserved among insect DGAT1, and also between insect and vertebrate DGAT1. Several of these sites are located in the N-terminal region. Interestingly, deletion of the N-terminal of the mouse DGAT1 renders the protein more active[83] suggesting that phosphorylation in this protein region could play an important regulatory role in the metabolism of TG. For instance, the adipokinetic hormone, AKH, is known to activate PKA and promote activation of lipolysis[84]. These events lead to the accumulation of DG in fat body and also a massive secretion of DG into the hemolymph[85]. It is possible that the large production of DG induced by AKH could be achieved by inhibition of DGAT1 upon PKA mediated phosphorylation. Clearly, further studies on the possible role of the predicted phosphorylation sites in the function of DGAT1 and the metabolism of TG in insects will be very interesting. The high conservation of DGAT1 between vertebrates and insects suggests that several properties of this enzyme could also be conserved. Human DGAT1 has also been shown to have MGAT activity and catalyze the synthesis of waxes, and retinyl esters. This could also be the case of DGAT1 from insects. The synthesis of waxes is very important to prevent dehydration by lowering the water permeability of the cuticle and eggs.

DGAT1-knockout mice are viable and fertile even though their phenotype shows major changes in lipid metabolism and energy homeostasis[86]. Thus, among other changes, mice lacking DGAT1 are leaner, more sensitive to insulin, and have dry fur apparently due to their deficiency in the synthesis of waxes [86]. Relevant studies on insect DGATs are limited to one report on an ethyl methanesulfonate generated Drosophila mutant. Female flies carrying mutations in the midway gene are sterile. The midway gene was shown to encode a DGAT1 and play a major role in the accumulation of TG in ovaries [33]. Mutations in the midway gene decrease the accumulation of TG in nurse cells and this has been suggested as the cause of early nurse cell degeneration and sterility[87].

This study shows that DGAT1 is expressed in the three major M. sexta organs that are known to store TG, such as ovaries[88], midgut [89] and fat body[6]. We have not studied other tissues, yet. However, DGAT1 is likely to be broadly expressed. The synthesis of pheromones in moths takes place in the pheromone gland (PG) using FAs as precursors; i.e. Bombykol is made from palmitic acid. DGAT1 should be highly expressed in the pheromone producing cells of female moths before maturity. At that time the PG shows an increase in lipid droplets due to the accumulation of TG[90]. In this regard, a recent study has shown that the expression of a "DGAT2" transcript in PG of Bombyx mori increases during the preparation for mating[91]. Our study suggests that the "BmDGAT2" gene actually encodes an MGAT-2 like protein. Therefore, the expression of both MGAT and DGAT 1 would be needed for the synthesis of TG in PG.

The developmental changes in the expression of MsexDGAT1 mRNA observed in this study suggest that the expression of DGAT1 in fat body is regulated according to the physiological needs of the insect. This was exemplified by the ~7-fold higher fat body levels of DGAT1 mRNA

in feeding larvae, which is accumulating TG, than in adult insects, which are mobilizing and burning fat. These changes suggest that DGAT1 could be a rate limiting enzyme in the synthesis of fat body TG. Regulation of the expression of DGAT1 is important because this enzyme catalyzes a metabolic step centered at the branch point where the metabolic fate of DG is at least temporarily defined. Conversion of DG to TG for storage reduces the availability of DG for phospholipid synthesis and for export to the hemolymph.

MGAT gene

The Manduca genome project suggested the presence of two MGAT transcripts coding for proteins of 346 and 352 amino acids. With the exception of the first nine N-terminal residues, these two proteins are identical. The transcripts shared identical 3'-UTR sequences but differed at the 5'-ends (UTR and 1st coding exon). To confirm the occurrence of these two transcripts we designed primers targeting the 5'-UTRs of the two isoforms and a primer targeting the common 3'-UTRs. PCR of fat body cDNA showed that both isoforms were expressed. Both full length transcripts were cloned and sequenced (gb accession # KF800699 and KF800700 for MsexMGAT_346 and 352, respectively). A comparison of the sequences obtained with the sequences of well characterized acyltransferases from human a mouse indicated that they are homologous of the vertebrates MGAT2. The figure22 shows an alignment of the deduced MsexMGAT protein sequences with those corresponding to human and mouse MGAT2. The MsexMGAT sequences were compared with 18 other similar proteins from insects and vertebrates. As shown in the identity matrix, Table 3, nearly all insect proteins homologous to MsexMGAT are more similar to human or mouse MGAT2 than to human or mouse DGAT2, MGAT1 or MGAT3. The single exception found was the MGAT from the ant Harpegnathos

saltator that is more similar to the vertebrates MGAT1 (Table 3). As it was the case for DGAT1, it is important to remark that some of the insect MGAT like proteins used in Table 3 are annotated as DGAT or DGAT2. This is the case for at least EHJ64327.1 (Danus plexipus) and XP 001653515.1 (Aedes aegypti). Clearly these proteins are more similar to MGATs than to DGAT2. An alignment of the 20 proteins also considered in this study. Human and mouse DGAT2 are distinguished from all MGATs by their longer non-matching N-terminal sequences. Prediction of the TMH of MsexMGAT also shows similarities with human MGAT2 and some differences with human DGAT2 (Figure 20). The two isoforms of MsexMGAT cloned appear to derive from a single gene. The structure of the gene indicates the presence of seven exons. The shorter form, MGAT346, is the product of exons 2-7, whereas MsexMGAT352 is the splicing product containing exons 1 and 4-7 (Figure 20).

	Msex MGAT346	**Msex MGAT352**	**Bm**	***BmDGAT2**	***Dp**	**Nv**	**Hs**	**Tc**	**Ag**	***Aae**	***DmCG1941**	***DmCG1942**	***DmCG1946**	**Human MGAT1**	**Mouse MGAT1**	**Human MGAT2**	**Mouse MGAT2**	**Human DGAT2**	**Mouse DGAT2**	**Human MGAT3**
Msex MGAT346	**100**	**99.1**	**78.3**	**78.6**	**71.6**	49.7	46.2	43.5	43.5	42.9	36.8	39.3	37.4	41.8	41.8	**44.6**	**44.3**	36.6	36.6	37.6
Msex MGAT352	**99.1**	**100**	**76.9**	**76.7**	**71.8**	49.7	46.2	43.5	43.5	42.9	36.8	39.3	37.4	41.8	41.8	**44.6**	**44.3**	35.7	35.7	37.6
Bm	**78.3**	**76.9**	**100**	**98.0**	**70.6**	50.6	46.8	44.6	46.8	45.6	39.2	41.1	38.9	41.5	42.4	**46.7**	**45.2**	37.4	37.7	40.3
*BmDGAT2	**78.6**	**76.7**	**98.0**	**100**	**70.4**	50.6	46.8	44.6	46.8	45.6	39.2	41.1	38.9	41.5	42.4	**46.7**	**45.2**	37.0	37.3	40.3
*Dp	**71.6**	**71.8**	**70.6**	**70.4**	**100**	50.0	47.9	44.1	47.0	45.9	37.4	40.2	40.1	39.1	39.7	**44.0**	**44.3**	35.5	34.7	37.9
Nv	49.7	49.7	50.6	50.6	50.0	100	57.2	45.2	43.6	47.3	38.6	39.0	38.1	40.6	41.2	**41.9**	**43.1**	39.1	39.6	37.0
Hs	46.2	46.2	46.8	46.8	47.9	57.2	100	47.6	41.6	41.9	34.1	36.6	36.5	**42.4**	40.3	41.0	40.4	38.8	39.1	36.4
Tc	43.5	43.5	44.6	44.6	44.1	45.2	47.6	100	41.9	41.9	35.1	38.9	37.9	40.4	40.1	**47.1**	**47.1**	37.9	37.9	37.4
Ag	43.5	43.5	46.8	46.8	47.0	43.6	41.6	41.9	100	67.1	42.6	42.2	41.8	39.7	37.6	**42.2**	**40.7**	35.1	35.1	34.4
*Aae	42.9	42.9	45.6	45.6	45.9	47.3	41.9	41.9	67.1	100	42.9	43.3	41.8	38.5	37.6	**42.2**	**42.5**	34.8	34.8	35.3
*Dm CG1941	36.8	36.8	39.2	39.2	37.4	38.6	34.1	35.1	42.6	42.9	100	72.9	67.1	34.0	35.2	**36.8**	**38.0**	33.7	34.0	36.0
*Dm CG1942	39.3	39.3	41.1	41.1	40.2	39.0	36.6	38.9	42.2	43.3	72.9	100	67.8	35.6	36.8	**39.0**	**39.0**	34.4	34.4	38.0
*Dm CG1946	37.4	37.4	38.9	38.9	40.1	38.1	36.5	37.9	41.8	41.8	67.1	67.8	100	34.6	36.8	**38.1**	**38.7**	32.5	32.5	36.1
Human MGAT1	41.8	41.8	41.5	41.5	39.1	40.6	42.4	40.4	39.7	38.5	34.0	35.6	34.6	100	72.5	53.0	52.1	48.7	48.1	43.2
Mouse MGAT1	41.8	41.8	42.4	42.4	39.7	41.2	40.3	40.1	37.6	37.6	35.2	36.8	36.8	72.5	100	53.0	52.7	45.7	45.1	40.8

Human MGAT2	44.6	44.6	46.7	46.7	44.0	41.9	41.0	47.1	42.2	42.2	36.8	39.0	38.1	53.0	53.0	100	81.1	45.8	45.5	46.4
Mouse MGAT2	44.3	44.3	45.2	45.2	44.3	43.1	40.4	47.1	40.7	42.5	38.0	39.0	38.7	52.1	52.7	81.1	100	46.4	46.7	46.39
Human DGAT2	36.6	35.7	37.4	37.0	35.5	39.1	38.8	37.9	35.1	34.8	33.7	34.4	32.5	48.7	45.7	45.8	46.4	100	95.1	49.9
Mouse DGAT2	36.6	35.7	37.7	37.3	34.7	39.6	39.1	37.9	35.1	34.8	34.0	34.4	32.5	48.1	45.1	45.5	46.7	95.1	100	50.2
Human MGAT3	37.6	37.6	40.3	40.3	37.9	37.0	36.4	37.4	34.4	35.3	36.0	38.0	36.1	43.2	40.8	46.4	46.4	49.9	50.2	100

Table3.

Identity matrix of insect, human and mouse proteins from the DGAT2 family: MsexMGAT346, gb: KF800699; MsexMGAT352, gb: KF800700; Bm: Bombyx mori MGAT2-like XP_004922894.1; BmDGAT2: Bombyx mori bgibmga008049-ta (Annotated as DGAT2); Dp: Danus plexipus, gb:EHJ64327.1 (Annotated as putative DGAT); Nv: Nasonia vitripennis MGAT2-like, XP_001602288.1; Hs: Harpegnathos saltator MGAT1, gb:EFN85928.1; Tc: Tribolium castaneum MGAT2, gb:EEZ98240.1; Ag: Anopheles gambiae, gb:EDO63767.1; Aae: Aedes aegypti, gb:EAT39311.1 (Annotated as DGAT); Dm: Drosophila melanogaster CG1941, CG1942 and CG1946 (Annotated as DGAT); Human MGAT1: NP_477513.2; Mouse MGAT1: NP_080989.2; Human MGAT2: NP_079374.2; Mouse MGAT2: Q80W94;Human DGAT2: Homo sapiens DGAT2 Isoform 1, NP_115953; Mouse DGAT2: NP_080660.1; Human MGAT3: NP_835470.

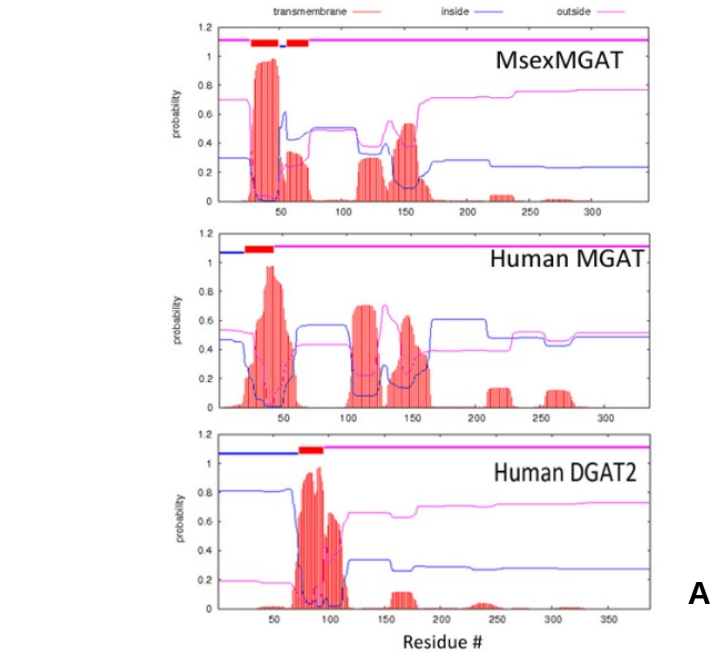

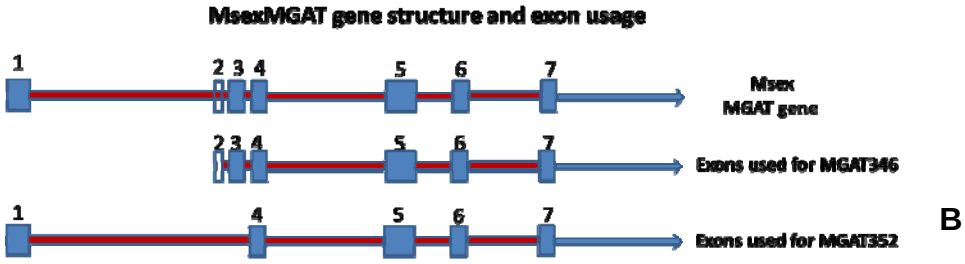

Figure 20. Features of MsexMGAT gene and protein structure. A) The number and location of transmembrane helices (TMH) was predicted using the tools from the Center for Biological Sequence Analysis (www.cbs.dtu.dk/services/TMHMM). Sequence IDs: MsexMGAT (KF800700), Human MGAT2 (NP_036211.2; GI 37537527) and Human DGAT2 (NP_115953.2). B) Gene structure and predicted exon usage for MsexMGAT346 and MsexMGAT352. As inferred from the Manduca genome

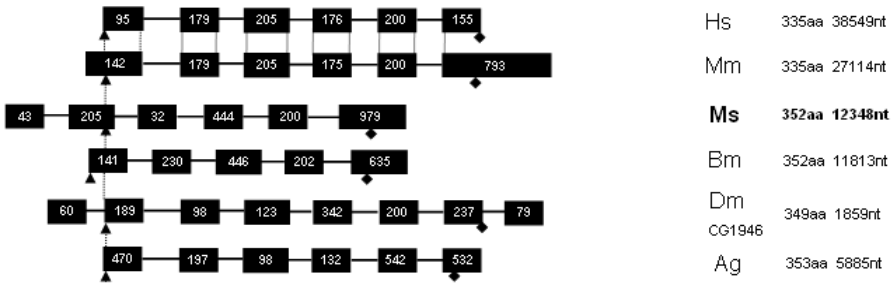

Figure 21. Structure of MGAT genes. The figure shows the gene length and the number and size of the exons for MGAT genes from several insect species. Also included are the structures of the MGAT genes found in mouse and human genomes. The number and size of the exons and the total gene lengths are indicated. The size of each exon (in bp) is given. Bars represent introns. Start site is marked with arrow head (▲) and stop codon is marked with diamond (◆).

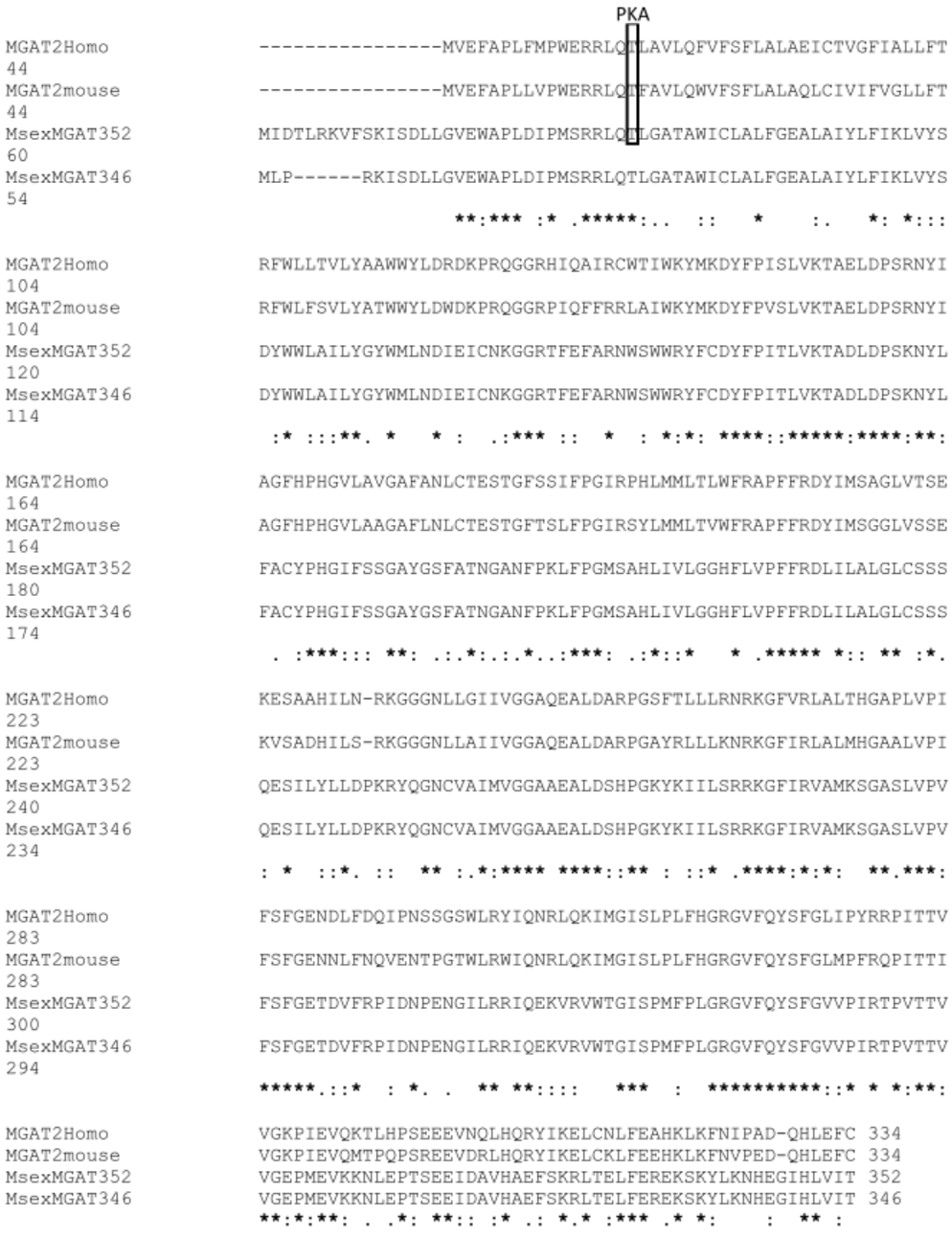

Fig. 22 Protein sequence alignment of Human and mouse MGAT2 and MsexMGATs.

Alignments were produced with Clustal Omega. Sequence IDs: Human MGAT2 :

NP_036211.2; Mouse MGAT2: Q80W94,MsexMGAT 352: KF800700, MsexMGAT 346: KF800699.

Three alternative pathways have been considered for the production of sn-1,2-DG in fat body: (1) the stereospecific hydrolysis of TG into sn-1,2-DG; (2) the hydrolysis of TG to sn-2-monoacylglycero1 (sn-2-MG), followed by stereospecific acylation of sn-2-MG and (3) de novo synthesis of DG from glycerol-3 phosphate via phosphatidic acid using the fatty acids produced by TG hydrolysis. The relative contribution of each of these possible pathways to the synthesis of DG in the fat body is not known, yet. Based on the fact that 2-MG is the main product of TG hydrolysis by the major fat body lipase[8], the MG-pathway was also suggested as a major route for the synthesis of DG in M. sexta fat body. Moreover, in vitro studies have characterized the MGAT activity of M. sexta fat body and shown that it produces sn-1,2-DG[11]. The MGAT activity of body has also been determined and characterized in L. migratoria and Periplaneta americana .

The two MsexMGATs cloned and all predicted insect MGAT proteins, with the exception of the Harpegnathos saltator MGAT, were more similar to the vertebrates' MGAT2 than to MGAT 1 and MGAT3. The MGAT3 gene is found only in higher mammals and humans but not in rodents[92] and, therefore, its absence in insects is not surprising. The higher similarity with MGAT2 may be related to the kinetic properties of the enzyme. MGAT2 is expressed in most tissues in vertebrates, but it is highly abundant in intestine[93], where the MG-pathway is prevalent. Therefore, it is possible that the similarity of insect MGATs with the vertebrates MGAT2 be due to the significance of the MG-pathway in the metabolism of neutral glycerides.

Conversely to MsexDGAT, the expression of MsexMGAT is up-regulated and shows the

maximum values in the adult stage. The changes in MGAT expression between the feeding larval and adult stages, a 2-fold change, are not as pronounced as observed for DGAT. However, the combined regulation of the expression of MGAT and DGAT leads to major changes between the

ratios of the expression levels of DGAT1/MGAT. Since up-regulation of MGAT is expected to increase the synthesis of DG whereas down-regulation of DGAT is expected to decrease the rate of TG synthesis, these simultaneous changes should lead to an increase in the net production and accumulation of DG in adult insects (TG in larvae). The fact that this is exactly what is observed, as shown by the incorporation of FA in glycerides suggests that MsexMGAT and DGAT are key enzymes defining whether the fat body stores TG or release DG into circulation. In other words, the present study suggests that the monoacylglycerol pathway constitutes a major pathway for the synthesis of DG.

Phylogeny of insect DGAT1 and MGAT proteins

Previous phylogenetic studies of acyltransferases have shown that DGAT1 and DGAT2 share little sequence homology and actually fall into different phylogenetic families. DGAT1 belongs to the family of MBOAT proteins, whereas DGAT2 and MGATs cluster in a group named the DGAT2 family [34, 94, 95]. In this report we have extended the phylogenetic study of neutral acyltranserases by analyzing the recently available DGAT and MGAT protein sequences deduced for M. sexta and several other insect homologous proteins described above. A phylogenetic tree comparing insect MGAT and DGAT1 proteins and their relationships with the well characterized human and murine proteins was conducted. As expected from previous studies[94], human MGAT and DGAT2 sequences grouped together into the so called human DGAT2 family of

acyltransferases. The DGAT2 family included all predicted insect MGAT proteins. Sub-clades distinguishing MGATs from different insect orders are clearly distinguished at least among Lepidoptera, Hymenoptera and Diptera. Dipteran MGATs, however, show divergence between Drosophila and mosquitoes.

On the other hand, all predicted insect DGAT1 proteins grouped together with vertebrates DGAT1 in a clade (MBOAT family) clearly separated from the DGAT2 family. This is consistent with the notion that MBOAT and DGAT2 families originated from different prokaryote ancestors[96]. Moreover, as observed for insect MGATs, the phylogenetic tree of DGAT1 also shows a clear separation of sub-clades according to the insect orders.

REFERENCES

1. Chamorro, S., et al., *Pollination patterns and plant breeding systems in the Galapagos: a review.* Ann Bot, 2012. **110**(7): p. 1489-501.
2. Engel, M.S. and D.A. Grimaldi, *New light shed on the oldest insect.* Nature, 2004. **427**(6975): p. 627-30.
3. Beenakkers, A.M., et al., *Insect adipokinetic hormones.* Peptides, 1985. **6 Suppl 3**: p. 437-44.
4. Beenakkers, A.M., D.J. Van der Horst, and W.J. Van Marrewijk, *Insect lipids and lipoproteins, and their role in physiological processes.* Prog Lipid Res, 1985. **24**(1): p. 19-67.
5. Jorgensen, R.J., et al., *Preventive anthelmintic treatment of grazing young cattle via supplementary feed and drinking water.* Vet Rec, 1987. **121**(20): p. 468-71.
6. Arrese, E.L. and J.L. Soulages, *Insect fat body: energy, metabolism, and regulation.* Annu Rev Entomol, 2010. **55**: p. 207-25.
7. Garda, H.A., E.L. Arrese, and J.L. Soulages, *Structure of apolipophorin-III in discoidal lipoproteins. Interhelical distances in the lipid-bound state and conformational change upon binding to lipid.* J Biol Chem, 2002. **277**(22): p. 19773-82.
8. Arrese, E.L. and M.A. Wells, *Purification and properties of a phosphorylatable triacylglycerol lipase from the fat body of an insect, Manduca sexta.* J Lipid Res, 1994. **35**(9): p. 1652-60.
9. Arrese, E.L., R.T. Patel, and J.L. Soulages, *The main triglyceride-lipase from the insect fat body is an active phospholipase A(1): identification and characterization.* J Lipid Res, 2006. **47**(12): p. 2656-67.
10. Arrese, E.L. and M.A. Wells, *Adipokinetic hormone-induced lipolysis in the fat body of an insect, Manduca sexta: synthesis of sn-1,2-diacylglycerols.* J Lipid Res, 1997. **38**(1): p. 68-76.
11. Arrese, E.L., B.I. Rojas-Rivas, and M.A. Wells, *Synthesis of sn-1,2-diacylglycerols by monoacylglycerol acyltransferase from Manduca sexta fat body.* Arch Insect Biochem Physiol, 1996. **31**(3): p. 325-35.
12. Patel, R.T., et al., *Activation of the lipid droplet controls the rate of lipolysis of triglycerides in the insect fat body.* J Biol Chem, 2005. **280**(24): p. 22624-31.

13. Patel, R.T., J.L. Soulages, and E.L. Arrese, *Adipokinetic hormone-induced mobilization of fat body triglyceride stores in Manduca sexta: role of TG-lipase and lipid droplets.* Arch Insect Biochem Physiol, 2006. **63**(2): p. 73-81.
14. Langin, D., et al., *Adipocyte lipases and defect of lipolysis in human obesity.* Diabetes, 2005. **54**(11): p. 3190-7.
15. Ryden, M., et al., *Comparative studies of the role of hormone-sensitive lipase and adipose triglyceride lipase in human fat cell lipolysis.* Am J Physiol Endocrinol Metab, 2007. **292**(6): p. E1847-55.
16. Miyoshi, H., et al., *Adipose triglyceride lipase regulates basal lipolysis and lipid droplet size in adipocytes.* J Cell Biochem, 2008. **105**(6): p. 1430-6.
17. Schweiger, M., et al., *Adipose triglyceride lipase and hormone-sensitive lipase are the major enzymes in adipose tissue triacylglycerol catabolism.* J Biol Chem, 2006. **281**(52): p. 40236-41.
18. Zimmermann, R., et al., *Fat mobilization in adipose tissue is promoted by adipose triglyceride lipase.* Science, 2004. **306**(5700): p. 1383-6.
19. Kershaw, E.E., et al., *Adipose triglyceride lipase: function, regulation by insulin, and comparison with adiponutrin.* Diabetes, 2006. **55**(1): p. 148-57.
20. Haemmerle, G., et al., *Defective lipolysis and altered energy metabolism in mice lacking adipose triglyceride lipase.* Science, 2006. **312**(5774): p. 734-7.
21. Lass, A., et al., *Adipose triglyceride lipase-mediated lipolysis of cellular fat stores is activated by CGI-58 and defective in Chanarin-Dorfman Syndrome.* Cell Metab, 2006. **3**(5): p. 309-19.
22. Miyoshi, H., et al., *Control of adipose triglyceride lipase action by serine 517 of perilipin A globally regulates protein kinase A-stimulated lipolysis in adipocytes.* J Biol Chem, 2007. **282**(2): p. 996-1002.
23. Granneman, J.G., et al., *Analysis of lipolytic protein trafficking and interactions in adipocytes.* J Biol Chem, 2007. **282**(8): p. 5726-35.
24. Wei, S., et al., *Retinyl ester hydrolysis and retinol efflux from BFC-1beta adipocytes.* J Biol Chem, 1997. **272**(22): p. 14159-65.
25. Clifford, G.M., et al., *Translocation of hormone-sensitive lipase and perilipin upon lipolytic stimulation of rat adipocytes.* J Biol Chem, 2000. **275**(7): p. 5011-5.
26. Bartz, R., et al., *Dynamic activity of lipid droplets: protein phosphorylation and GTP-mediated protein translocation.* J Proteome Res, 2007. **6**(8): p. 3256-65.
27. Villena, J.A., et al., *Desnutrin, an adipocyte gene encoding a novel patatin domain-containing protein, is induced by fasting and glucocorticoids: ectopic expression of desnutrin increases triglyceride hydrolysis.* J Biol Chem, 2004. **279**(45): p. 47066-75.
28. Bezaire, V., et al., *Contribution of adipose triglyceride lipase and hormone-sensitive lipase to lipolysis in hMADS adipocytes.* J Biol Chem, 2009. **284**(27): p. 18282-91.
29. Kennedy, E.P., *Metabolism of lipides.* Annu Rev Biochem, 1957. **26**: p. 119-48.
30. Bell, R.M. and R.A. Coleman, *Enzymes of glycerolipid synthesis in eukaryotes.* Annu Rev Biochem, 1980. **49**: p. 459-87.
31. Lehner, R. and A. Kuksis, *Biosynthesis of triacylglycerols.* Prog Lipid Res, 1996. **35**(2): p. 169-201.

32. Coleman, R.A., et al., *Do long-chain acyl-CoA synthetases regulate fatty acid entry into synthetic versus degradative pathways?* J Nutr, 2002. **132**(8): p. 2123-6.
33. Xia, T., et al., *Selective retention of essential fatty acids: the role of hepatic monoacylglycerol acyltransferase.* Am J Physiol, 1993. **265**(2 Pt 2): p. R414-9.
34. Yen, C.L., et al., *Thematic review series: glycerolipids. DGAT enzymes and triacylglycerol biosynthesis.* J Lipid Res, 2008. **49**(11): p. 2283-301.
35. Kwanyuen, P. and R.F. Wilson, *Subunit and amino acid composition of diacylglycerol acyltransferase from germinating soybean cotyledons.* Biochim Biophys Acta, 1990. **1039**(1): p. 67-72.
36. Hobbs, D.H. and M.J. Hills, *Expression and characterization of diacylglycerol acyltransferase from Arabidopsis thaliana in insect cell cultures.* Biochem Soc Trans, 2000. **28**(6): p. 687-9.
37. Lok, C.M. and D.J. van der Horst, *Chiral 1,2-diacylglycerols in the haemolymph of the locust, Locusta migratoria.* Biochim Biophys Acta, 1980. **618**(1): p. 80-7.
38. Kamagate, A. and H.H. Dong, *FoxO1 integrates insulin signaling to VLDL production.* Cell Cycle, 2008. **7**(20): p. 3162-70.
39. Jiang, Z., et al., *Pattern profiling and mapping of the fat body transcriptome in Drosophila melanogaster.* Obes Res, 2005. **13**(11): p. 1898-904.
40. Hansen, I.A., et al., *Target of rapamycin-dependent activation of S6 kinase is a central step in the transduction of nutritional signals during egg development in a mosquito.* J Biol Chem, 2005. **280**(21): p. 20565-72.
41. Brasaemle, D.L., *Thematic review series: adipocyte biology. The perilipin family of structural lipid droplet proteins: stabilization of lipid droplets and control of lipolysis.* J Lipid Res, 2007. **48**(12): p. 2547-59.
42. Brasaemle, D.L., *Lipolysis control: the plot thickens.* Cell Metab, 2010. **11**(3): p. 173-4.
43. Arrese, E.L., et al., *Mobilization of lipid stores in Manduca sexta: cDNA cloning and developmental expression of fat body triglyceride lipase, TGL.* Insect Biochem Mol Biol, 2010. **40**(2): p. 91-9.
44. Inoue, H., et al., *Roles of SAM and DDHD domains in mammalian intracellular phospholipase A1 KIAA0725p.* Biochim Biophys Acta, 2012. **1823**(4): p. 930-9.
45. Aravind, L., *The WWE domain: a common interaction module in protein ubiquitination and ADP ribosylation.* Trends Biochem Sci, 2001. **26**(5): p. 273-5.
46. Zweifel, M.E., D.J. Leahy, and D. Barrick, *Structure and Notch receptor binding of the tandem WWE domain of Deltex.* Structure, 2005. **13**(11): p. 1599-611.
47. Merchant, S.S., et al., *The Chlamydomonas genome reveals the evolution of key animal and plant functions.* Science, 2007. **318**(5848): p. 245-50.
48. Bednarova, A., D. Kodrik, and N. Krishnan, *Adipokinetic hormone exerts its anti-oxidative effects using a conserved signal-transduction mechanism involving both PKC and cAMP by mobilizing extra- and intracellular Ca2+ stores.* Comp Biochem Physiol C Toxicol Pharmacol, 2013. **158**(3): p. 142-9.
49. Arrese, E.L., et al., *Function and structure of lipid storage droplet protein 1 studied in lipoprotein complexes.* Arch Biochem Biophys, 2008. **473**(1): p. 42-7.
50. Auerswald, L. and G. Gade, *Endocrine control of TAG lipase in the fat body of the migratory locust, Locusta migratoria.* Insect Biochem Mol Biol, 2006. **36**(10):

p. 759-68.
51. Auerswald, L., K.J. Siegert, and G. Gade, *Activation of triacylglycerol lipase in the fat body of a beetle by adipokinetic hormone.* Insect Biochem Mol Biol, 2005. **35**(5): p. 461-70.
52. Bernbom, N., et al., *Adhesion of food-borne bacteria to stainless steel is reduced by food conditioning films.* J Appl Microbiol, 2009. **106**(4): p. 1268-79.
53. Whitmore, L. and B.A. Wallace, *Protein secondary structure analyses from circular dichroism spectroscopy: methods and reference databases.* Biopolymers, 2008. **89**(5): p. 392-400.
54. Soulages, J.L., et al., *Developmental changes in the protein composition of Manduca sexta lipid droplets.* Insect Biochem Mol Biol, 2012. **42**(5): p. 305-20.
55. Matuda, S. and T. Saheki, *Intracellular distribution and biosynthesis of lipoamide dehydrogenase in rat liver.* J Biochem, 1982. **91**(2): p. 553-61.
56. Pullikuth, A.K. and S.S. Gill, *Primary structure of an invertebrate dihydrolipoamide dehydrogenase with phylogenetic relationship to vertebrate and bacterial disulfide oxidoreductases.* Gene, 1997. **200**(1-2): p. 163-72.
57. Danson, M.J., *Dihydrolipoamide dehydrogenase: a 'new' function for an old enzyme?* Biochem Soc Trans, 1988. **16**(2): p. 87-9.
58. Danson, M.J., et al., *Dihydrolipoamide dehydrogenase from Trypanosoma brucei. Characterization and cellular location.* Biochem J, 1987. **243**(3): p. 661-5.
59. Portela, M.P. and A.O. Stopopani, *Lipoamide dehydrogenase from Trypanosoma cruzi: some properties and cellular localization.* Biochem Int, 1991. **24**(1): p. 147-55.
60. Schafer, F.Q. and G.R. Buettner, *Redox environment of the cell as viewed through the redox state of the glutathione disulfide/glutathione couple.* Free Radic Biol Med, 2001. **30**(11): p. 1191-212.
61. Kanzok, S.M., et al., *Substitution of the thioredoxin system for glutathione reductase in Drosophila melanogaster.* Science, 2001. **291**(5504): p. 643-6.
62. Igamberdiev, A.U., et al., *Dihydrolipoamide dehydrogenase from porcine heart catalyzes NADH-dependent scavenging of nitric oxide.* FEBS Lett, 2004. **568**(1-3): p. 146-50.
63. Hansen, R.E., D. Roth, and J.R. Winther, *Quantifying the global cellular thiol-disulfide status.* Proc Natl Acad Sci U S A, 2009. **106**(2): p. 422-7.
64. Kil, I.S. and J.W. Park, *Regulation of mitochondrial NADP+-dependent isocitrate dehydrogenase activity by glutathionylation.* J Biol Chem, 2005. **280**(11): p. 10846-54.
65. Becker, K. and R.H. Schirmer, *1,3-Bis(2-chloroethyl)-1-nitrosourea as thiol-carbamoylating agent in biological systems.* Methods Enzymol, 1995. **251**: p. 173-88.
66. Arscott, L.D., et al., *The mechanism of thioredoxin reductase from human placenta is similar to the mechanisms of lipoamide dehydrogenase and glutathione reductase and is distinct from the mechanism of thioredoxin reductase from Escherichia coli.* Proc Natl Acad Sci U S A, 1997. **94**(8): p. 3621-6.
67. Angelucci, F., et al., *Inhibition of Schistosoma mansoni thioredoxin-glutathione reductase by auranofin: structural and kinetic aspects.* J Biol Chem, 2009. **284**(42): p. 28977-85.

68. Argyrou, A. and J.S. Blanchard, *Mycobacterium tuberculosis lipoamide dehydrogenase is encoded by Rv0462 and not by the lpdA or lpdB genes.* Biochemistry, 2001. **40**(38): p. 11353-63.
69. Dalle-Donne, I., et al., *Protein S-glutathionylation: a regulatory device from bacteria to humans.* Trends Biochem Sci, 2009. **34**(2): p. 85-96.
70. Huo, J., et al., *Cloning and purification of recombinant silkworm dihydrolipoamide dehydrogenase expressed in Escherichia coli.* Protein Expr Purif, 2010. **72**(1): p. 95-100.
71. Van Heusden, M.C. and J.H. Law, *An insect lipid transfer particle promotes lipid loading from fat body to lipoprotein.* J Biol Chem, 1989. **264**(29): p. 17287-92.
72. Van der Horst, D.J., S.D. Roosendaal, and K.W. Rodenburg, *Circulatory lipid transport: lipoprotein assembly and function from an evolutionary perspective.* Mol Cell Biochem, 2009. **326**(1-2): p. 105-19.
73. van der Horst, D.J., et al., *Alternative lipid mobilization: the insect shuttle system.* Mol Cell Biochem, 2002. **239**(1-2): p. 113-9.
74. Canavoso, L.E., et al., *Lipid transfer particle mediates the delivery of diacylglycerol from lipophorin to fat body in larval Manduca sexta.* J Lipid Res, 2004. **45**(3): p. 456-65.
75. Van Hoof, D., K.W. Rodenburg, and D.J. Van der Horst, *Receptor-mediated endocytosis and intracellular trafficking of lipoproteins and transferrin in insect cells.* Insect Biochem Mol Biol, 2005. **35**(2): p. 117-28.
76. Soulages, J.L., et al., *Hydration and localization of diacylglycerol in the insect lipoprotein lipophorin. A 13C-NMR study.* Biochemistry, 1994. **33**(11): p. 3245-51.
77. Rani, S.H., S. Saha, and R. Rajasekharan, *A soluble diacylglycerol acyltransferase is involved in triacylglycerol biosynthesis in the oleaginous yeast Rhodotorula glutinis.* Microbiology, 2013. **159**(Pt 1): p. 155-66.
78. Thompson, J.D., D.G. Higgins, and T.J. Gibson, *CLUSTAL W: improving the sensitivity of progressive multiple sequence alignment through sequence weighting, position-specific gap penalties and weight matrix choice.* Nucleic Acids Res, 1994. **22**(22): p. 4673-80.
79. Liu, Q., et al., *Acyl-CoA:diacylglycerol acyltransferase: molecular biology, biochemistry and biotechnology.* Prog Lipid Res, 2012. **51**(4): p. 350-77.
80. Cheng, D., et al., *Acylation of acylglycerols by acyl coenzyme A:diacylglycerol acyltransferase 1 (DGAT1). Functional importance of DGAT1 in the intestinal fat absorption.* J Biol Chem, 2008. **283**(44): p. 29802-11.
81. Yen, C.L., et al., *The triacylglycerol synthesis enzyme DGAT1 also catalyzes the synthesis of diacylglycerols, waxes, and retinyl esters.* J Lipid Res, 2005. **46**(7): p. 1502-11.
82. Harris, C.A., et al., *DGAT enzymes are required for triacylglycerol synthesis and lipid droplets in adipocytes.* J Lipid Res, 2011. **52**(4): p. 657-67.
83. McFie, P.J., et al., *Topological orientation of acyl-CoA:diacylglycerol acyltransferase-1 (DGAT1) and identification of a putative active site histidine and the role of the n terminus in dimer/tetramer formation.* J Biol Chem, 2010. **285**(48): p. 37377-87.
84. Arrese, E.L., et al., *Calcium and cAMP are second messengers in the adipokinetic*

hormone-induced lipolysis of triacylglycerols in Manduca sexta fat body. J Lipid Res, 1999. **40**(3): p. 556-64.
85. Arrese, E.L., et al., *Diacylglycerol transport in the insect fat body: evidence of involvement of lipid droplets and the cytosolic fraction.* J Lipid Res, 2001. **42**(2): p. 225-34.
86. Smith, S.J., et al., *Obesity resistance and multiple mechanisms of triglyceride synthesis in mice lacking Dgat.* Nat Genet, 2000. **25**(1): p. 87-90.
87. Buszczak, M., et al., *Mutations in the midway gene disrupt a Drosophila acyl coenzyme A: diacylglycerol acyltransferase.* Genetics, 2002. **160**(4): p. 1511-8.
88. Ziegler, R. and R. Van Antwerpen, *Lipid uptake by insect oocytes.* Insect Biochem Mol Biol, 2006. **36**(4): p. 264-72.
89. Canavoso, L.E. and M.A. Wells, *Metabolic pathways for diacylglycerol biosynthesis and release in the midgut of larval Manduca sexta.* Insect Biochem Mol Biol, 2000. **30**(12): p. 1173-80.
90. Fonagy, A., N. Yokoyama, and S. Matsumoto, *Physiological status and change of cytoplasmic lipid droplets in the pheromone-producing cells of the silkmoth, Bombyx mori (Lepidoptera, Bombycidae).* Arthropod Struct Dev, 2001. **30**(2): p. 113-23.
91. Du, M., et al., *Identification of a diacylglycerol acyltransferase 2 gene involved in pheromone biosynthesis activating neuropeptide stimulated pheromone production in Bombyx mori.* J Insect Physiol, 2012. **58**(5): p. 699-703.
92. Cheng, D., et al., *Identification of acyl coenzyme A:monoacylglycerol acyltransferase 3, an intestinal specific enzyme implicated in dietary fat absorption.* J Biol Chem, 2003. **278**(16): p. 13611-4.
93. Cao, J., et al., *Cloning and functional characterization of a mouse intestinal acyl-CoA:monoacylglycerol acyltransferase, MGAT2.* J Biol Chem, 2003. **278**(16): p. 13860-6.
94. Cases, S., et al., *Cloning of DGAT2, a second mammalian diacylglycerol acyltransferase, and related family members.* J Biol Chem, 2001. **276**(42): p. 38870-6.
95. Lardizabal, K.D., et al., *DGAT2 is a new diacylglycerol acyltransferase gene family: purification, cloning, and expression in insect cells of two polypeptides from Mortierella ramanniana with diacylglycerol acyltransferase activity.* J Biol Chem, 2001. **276**(42): p. 38862-9.
96. Turchetto-Zolet, A.C., et al., *Evolutionary view of acyl-CoA diacylglycerol acyltransferase (DGAT), a key enzyme in neutral lipid biosynthesis.* BMC Evol Biol, 2011. **11**: p. 263.

VITA

Zengying Wu

Candidate for the Degree of

Doctor of Philosophy

Thesis: CHARACTERIZATION OF TRIACYLGLYCERIDE LIPASE AND MONO- AND DIACYLGLYCEROL ACYLTRANSFERASE IN *MANDUCA SEXTA*

Major Field: Biochemistry and Molecular Biology

Biographical:

Education:

Completed the requirements for the Doctor of Philosophy in Biochemistry and Molecular Biology at Oklahoma State University, Stillwater, Oklahoma in July, 2014.

Completed the requirements for the Master of Medicine in Medicine at Nankai University, Tianjin, China in 2009.

Completed the requirements for the Bachelor of Medicine in Medicine at Nankai University, Tianjin, China in 2009.